Check for updates

Circulation Research

ORIGINAL RESEARCH

T-World Virtual Human Cardiomyocyte. I. Development, Validation, and Cell Arrhythmogenesis

Jakub Tomek, Maxx Holmes, Thomas Bury, Marketa Tomkova, Heeseung Jo, Norbert Nagy, Ambre Bertrand, Alfonso Bueno-Orovio, Michael A. Colman, Blanca Rodriguez,* Donald M. Bers,* Jordi Heijman*

BACKGROUND: Cardiovascular disease is the leading global cause of morbidity and mortality. New technologies are needed to improve mechanistic understanding and inform therapeutic strategies. Human-centric cardiac simulations show great promise; however, existing cellular models can reproduce only a few arrhythmia-driving behaviors and show important discrepancies with experimental data. We aimed to develop a new model overcoming this lack of generality, which markedly limits the predictivity and translational utility of virtual cardiomyocytes.

METHODS: We developed T-World, a novel virtual human cardiomyocyte, using data-driven differential equations to describe sex-specific excitation-contraction coupling, mechanical contraction, β-adrenergic signaling, and its effects on cellular targets. The model contains several key innovations, including a new approach to coupling L-type calcium channels and ryanodine receptors, with updated calcium-dependent-inactivation of the former and novel calcium-induced refractoriness and complete reparameterization of the latter. We also redeveloped the sodium-potassium pump and made major improvements to the sodium-calcium exchanger formulation.

RESULTS: T-World shows broad agreement with experimental data on rate-dependent action potential (AP), calcium handling, and contraction properties. Extensively validated on independent data, T-World demonstrates strong predictive performance, for example, in drug-induced AP changes. The model reproduces the effects of sympathetic stimulation, including AP duration shortening and increased calcium-transient amplitude and contractility. Importantly, it recapitulates for the first time all key cellular mechanisms driving life-threatening arrhythmias (early and delayed afterdepolarizations, alternans, and steep S1-S2 restitution), including experimentally observed responses to interventions such as sympathetic activation, SERCA (sarco/endoplasmic reticulum Ca^{2+} ATPase) inhibition, and AP prolongation. Combined with the model's ability to simulate physiological sex-specific differences in electrophysiology, this revealed increased proclivity of female cardiomyocytes to early afterdepolarizations and steep restitution of AP duration.

CONCLUSIONS: T-World is a highly general and predictive open-source computer model of a human ventricular cardiomyocyte, suitable for multiscale research studies investigating determinants of arrhythmogenesis.

GRAPHIC ABSTRACT: A graphic abstract is available for this article.

Key Words: action potentials ■ arrhythmias, cardiac ■ cardiovascular diseases ■ morbidity ■ myocytes, cardiac

Circulation Research NOT FOR SALE ONLY

Downloaded from http://ahajournals.org by on April 7, 2026

Computational modeling and simulations of cardiac cellular and organ physiology have become an integral part of contemporary cardiovascular research, providing insights into basic physiological mechanisms and mechanisms of arrhythmia.[1] Moreover, these models of human cardiac (patho)physiology

Correspondence to: Jakub Tomek, DPhil, Department of Anatomy, Physiology, and Genetics, University of Oxford, Sherrington Bldg, OX1 3PT, Oxford, United Kingdom. Email jakub.tomek.mff@gmail.com
*B. Rodriguez, D.M. Bers, and J. Heijman are joint supervisors.
Supplemental Material is available at https://www.ahajournals.org/doi/suppl/10.1161/CIRCRESAHA.125.328073.
© 2026 The Authors. *Circulation Research* is published on behalf of the American Heart Association, Inc., by Wolters Kluwer Health, Inc. This is an open access article under the terms of the Creative Commons Attribution License, which permits use, distribution, and reproduction in any medium, provided that the original work is properly cited.
Circulation Research is available at www.ahajournals.org/journal/res

ORIGINAL RESEARCH

Novelty and Significance

What Is Known?

- Computer models of human cardiomyocytes (virtual cardiomyocytes) are an increasingly prioritized technology in academia and industry.
- Existing virtual cardiomyocytes can only reproduce a limited number of cellular arrhythmia mechanisms and show major discrepancies with experimental knowledge.
- This markedly limits their utility for studying interactions of different mechanisms and disease pathways.

What New Information Does This Article Contribute?

- We developed T-World, a human ventricular myocyte showing comprehensive agreement with human physiology, which can simulate all key arrhythmia-driving behaviors within a single framework.
- T-World integrates excitation-contraction coupling, sympathetic nervous signaling, and sex differences, indicating a novel sex-specific arrhythmia risk in females.
- The model was extensively validated on unseen data, showing strong predictive performance against independent experimental data sets, including drug responses and modulation of SERCA (sarco/endoplasmic reticulum Ca^{2+} ATPase) activity.

Computational models of human ventricular cardiomyocytes are increasingly used to study arrhythmia mechanisms and to support drug development, yet existing models typically capture only isolated aspects of cardiac pathophysiology. This study introduces T-World, a highly general computer model of the human cardiomyocyte that integrates electrophysiology, calcium handling, mechanical contraction, β-adrenergic signaling, and sex differences within a single coherent framework. For the first time, one model reproduces all major cellular arrhythmogenic mechanisms under experimentally relevant conditions while maintaining quantitative agreement with independent human data. By combining mechanistic rigor with extensive validation, T-World overcomes longstanding trade-offs between physiological accuracy and arrhythmia capability that limited prior models. The model also provides new insight into sex-specific arrhythmic vulnerability, suggesting steeper restitution and greater early afterdepolarization susceptibility in female myocytes. These advances establish T-World as a broadly applicable platform for mechanistic discovery, drug safety testing, disease modeling, and future multiscale simulations, thereby enhancing the translational potential of human-centric cardiac simulations and potentially reducing reliance on animal experimentation.

FIRST PROOF ONLY

Nonstandard Abbreviations and Acronyms

[ICaL]	L-type calcium channel
AP	action potential
APD	action potential duration
CaMKII	calcium/calmodulin-dependent protein kinase-II)
CaT	calcium transient
DAD	delayed afterdepolarization
EAD	early afterdepolarization
NCX	sodium-calcium exchanger
RyR	ryanodine receptor
SERCA	sarco/endoplasmic reticulum Ca^{2+} ATPase
SR	sarcoplasmic reticulum
TP06	Ten Tusscher-Panfilov 2006 model
βAR	beta-adrenergic

are increasingly used in therapy guidance,[2] and drug safety assessment.[3,4]

Computational modeling and simulations also hold tremendous potential for reducing, replacing, and refining the use of animals in research (3R principles). Although some animal-based studies in cardiac research are indispensable, simulations can minimize animal use by guiding experimental design, predicting outcomes, and aiding interpretation. Human-specific virtual cells can also predict functional implications of animal data in the context of human physiology, addressing critical species differences that may, for example, make a drug safe in mice but dangerous in humans.[5] Correspondingly, the European Medicines Agency, Food and Drug Administration, and UK government have recognized computational modeling as a key trend in advancing 3R principles.[6–8]

Multiple successful models of human ventricular cardiomyocytes have been developed to investigate specific mechanisms of cardiac (patho)physiology and arrhythmogenesis. The Rudy-family models (ORd and ToR-ORd) excel at predicting drug responses and generating early afterdepolarizations (EADs) under realistic conditions, making them valuable for drug safety and efficacy assessment.[3,4] The Bers/Grandi family models, for example, the recent model by Morotti et al (Morotti2021) used to study interspecies differences, are known for realistic calcium handling.[9–11] The Ten Tusscher-Panfilov 2006 model (TP06) is widely used to study arrhythmia related to restitution properties.[12] Despite their strengths, each

Downloaded from http://ahajournals.org by on April 7, 2026

model family lacks generality, capturing only a small subset of arrhythmic behaviors and manifesting important discrepancies with experimental data on fundamental physiology. This limits their utility for mechanistic studies, analyzing multifactorial drug effects, modeling complex diseases such as type 2 diabetes and heart failure, or integrative arrhythmia studies. Cardiomyocytes and their models are highly complex and include numerous components connected through nonlinear feedback loops. As a result, flaws in one model component can cascade, leading to incorrect predictions in other components and behaviors. This limits the predictive power and usefulness of previous models beyond their original focus. At the same time, the most innovative and relevant applications often arise precisely in these out-of-domain contexts. The lack of generality is in part also why different cellular models have typically been used to study aspects of arrhythmogenesis at cellular versus organ levels.[1]

The absence of a comprehensive and physiologically accurate virtual cardiomyocyte impedes progress toward translational applications and expanding the context of use of cardiac simulations. To address this gap and unlock the full potential of cardiac simulations in research, industry, and clinics, we aimed to develop a unified, highly general virtual cardiomyocyte. The generality should include (1) accurate recapitulation of human cellular cardiac physiology and its modulation by drugs or physiological changes, (2) the capability to manifest all key arrhythmogenic behaviors in conditions used to provoke them experimentally. This comprises EADs and delayed afterdepolarizations (DADs),[13,14] alternans,[15] and steep restitution of action potentials (APs),[16] (3) show suitability for multiscale modeling, enabling organ-level simulations.

In the first of 2 back-to-back articles, we present T-World, a novel virtual human cardiomyocyte that reproduces for the first time all key arrhythmogenic mechanisms while maintaining physiological accuracy across diverse conditions. Comparison to independent data not used in model creation demonstrates robust predictive accuracy at a broad range of tasks. T-World integrates electrophysiology, calcium handling, cardiomyocyte contraction, sympathetic stimulation, and sex differences, enabling comprehensive studies of their interactions. T-World is freely available via Matlab and CellML, with a free-to-use online graphical interface for noncoders (also runnable in Python). The second article on T-World demonstrates its utility for organ-scale simulations, pharmacological studies, and novel insights into disease mechanisms.[17]

METHODS

Data and Source Code Availability

T-World is distributed as open-source code and is available at https://github.com/jtmff/TWorld, including sample scripts demonstrating its functionality. An online graphical user interface enabling running T-World simulations is available at https://t-world-simulator-multipage-production.up.railway.app/. Background of the T-World development, including the description of various dead ends that we encountered during development, will be provided at the blog underlid.blogspot.com.

T-World is a virtual cell model using sets of ordinary differential equations to describe, based on experimental data, the dynamics of ionic currents, fluxes, and subcellular signaling. The overall cell architecture and calcium handling were mainly inspired by the Bers/Grandi family of models,[9–11] with most ionic current formulations inspired by the ToR-ORd model.[4]

To enable all key arrhythmic behaviors under relevant experimental conditions, and to avoid limitations of preceding frameworks with regard to basic physiological behaviors and response to (patho)physiological changes, we introduced developments across nearly every component of the cell, including ionic currents, calcium handling, and autonomic signaling. Among other changes, T-World includes (1) a new scheme of coupling L-type calcium channels and RyRs (ryanodine receptors), (2) addition of a calcium-dependent-inactivation gate for the L-type calcium channel and reformulation of the model around this change, including adaptations to the modeling of the driving force for calcium ions passing the membrane; (3) novel calcium-induced refractoriness and extensive reparameterization of the RyR model; (4) altered voltage dependence of the sodium-potassium pump, based on reassessment of data sources; (5) major improvement of a prior, well-established NCX (sodium-calcium exchanger) formulation, enabling appropriate simulation of the effects of sodium overload; and (6) development of a representation of the effects of sympathetic nervous signaling on the heart, for example, adding modulation of the contractile apparatus by this pathway. These core innovations enable realistic calcium dynamics and arrhythmogenic behaviors (see Results), solving limitations that persisted in the field for decades.

It should be noted that these advances are not superficial updates and that obtaining a model that combines the strengths of previous models without their limitations represents a major technical and conceptual difficulty. In complex, nonlinear systems like cardiac cells, direct combinations often introduce critical errors because models of cellular components are pushed beyond their intended use. T-World succeeds because of innovative integration strategies, rigorous validation, and the development of mechanistic modules, described in detail in the Supplemental Methods.

The model was developed through iterative interactions between human-driven biophysical understanding and automated multiobjective optimization. For example, model structures for new components were initially guided by experimental insights, followed by numerical optimization of the structure's parameters and subsequent analysis of model performance, leading to further adjustments and optimization of the model structure based on our understanding of the strengths and weaknesses of the formulation. Multiobjective genetic algorithms were used to fit parameters of single model components, as well as for integrating components. In these algorithms, a range of protocols would be simulated with a candidate model, with the simulation outputs compared with reference values based on experimental data. Detailed considerations, including the dimension of the objective function, population size, and number of iterations, as well as the exact formulation of the

Circulation Research FIRST PROOF ONLY

Downloaded from http://ahajournals.org by on April 7, 2026

final fitness functions used, are described in the Supplemental Methods.

The World in the model's name reflects the fact that model designs and expertise from the whole world were essential in its creation, and it goes beyond outputs of a single group, while the T stands for the last name of the first author, who brought this expertise together and was the driving force behind the model's development.

Please see Supplemental Methods for a detailed description of the following:

1. Model architecture.
2. Calibration and validation criteria for T-World development and evaluation.
3. Description of equations describing the ionic currents and fluxes (Figures S1 through S3).
4. Contractility representation (Figure S4).
5. CaMKII (calcium/calmodulin-dependent protein kinase-II) and βAR (beta-adrenergic) signaling (Figure S5).
6. Sex differences.
7. Methodology for studies on arrhythmogenic behaviors.
8. Graphical user interface.
9. Notes on implementation.
10. Sources of implementation of other models.

Statistics

The computational models used in this study are deterministic models that, for a given set of conditions, will always produce the same steady-state output. As such, no error bars can be shown for baseline model output, and statistical comparisons between the output of 2 model instances are not possible. Similarly, no statistical comparisons of model populations are provided, as the number of model instances that can be evaluated is arbitrarily large, resulting in arbitrarily small CIs for the point estimates of the model output. Assessment of the relative performance of different models and variants is based on whether key qualitative behaviors and features are reproduced or not, and on visual assessment of the provided model outputs and experimental data.

RESULTS

Model Overview and Key Outputs: AP, Calcium Transient, and Force

Based on extensive experimental data, the T-World model incorporates a broad range of ionic currents and fluxes across distinct cellular compartments, as well as subcellular signaling pathways and contractility (see Figure 1A for a high-level overview). Distinct model components are described by sets of ordinary differential equations, constructed to recapitulate baseline experimental data on single ionic currents and other cellular elements. Coupling all those components together yields a virtual cardiomyocyte.

The 3 key outputs of a cardiomyocyte model are its AP, calcium transient (CaT), and the resulting active tension during contraction. T-World shows a strong agreement with human AP data[18] with regards to AP duration (APD), resting membrane potential, and the overall shape of the AP during plateau and recovery (Figure 1B). It is in better agreement with human AP shape than most prior state-of-the-art models (Figure S6). The T-World CaT is also in excellent agreement with human data on time to peak, duration, and amplitude[19] (Figure 1C). T-World incorporates the Land model of contraction[21] as in the work of Margara et al,[20] and its mechanics outputs are fully consistent with experimental data on time to peak force, amplitude, and time to 95% recovery of contraction in human myocardium[20] (Figure 1D) while maintaining fundamental properties such as the cellular equivalent of the Frank-Starling law present in the Land model.

A given AP shape can be achieved through various combinations and balances of underlying currents.[22] The balance of key ionic currents in T-World was validated by simulating its exposure to 4 simulated channel-blocking drugs at 3 pacing rates (Figure 1E). T-World retains the strong predictive performance of ToR-ORd, showing excellent agreement with human data despite having a different cell architecture and calcium handling (Figure S7), predisposing T-World to applications in safety pharmacology. The Morotti2021 model is also mostly in agreement with the data at the more physiological heart rates (1–2 Hz), whereas the TP06 model shows substantial discrepancies with the experimental data (Figure S7).

Excitation-Contraction Coupling

Calcium-induced calcium release in cardiomyocytes involves calcium entering the cell via L-type calcium channels (I_{CaL}), which activate RyR on the sarcoplasmic reticulum (SR) to release additional calcium. Different models represent this process in distinct ways, each with specific strengths and limitations.

Models like ORd and ToR-ORd couple RyR release flux directly to I_{CaL}, yielding a realistic CaT shape, but this is mechanistically unrealistic and prevents spontaneous calcium release and DADs arising from RyR dysfunction or calcium overload. In contrast, Bers/Grandi–like models, including Morotti2021, base RyR opening on local calcium concentrations, which is mechanistically accurate, but causes delayed SR calcium release, as shown below. To address these limitations, T-World uses a hybrid approach. A small subset of RyR channels is I_{CaL}-dependent (representing the most closely associated I_{CaL} and RyR clusters), providing early calcium influx that primes the larger, calcium-sensitive RyR population, that are based on a revised version of the Shannon/Grandi RyR. This yields well-timed calcium-induced calcium release that is both calcium-sensitive and capable of generating DADs.

Despite different calcium-handling mechanisms, T-World's CaT kinetics are similar to ToR-ORd (Figure 2A). Both show a linear CaT upstroke with a small delay relative to the AP upstroke, matching experimental

Circulation Research
FIRST LOOK ONLY

Downloaded from http://ahajournals.org by on April 7, 2026

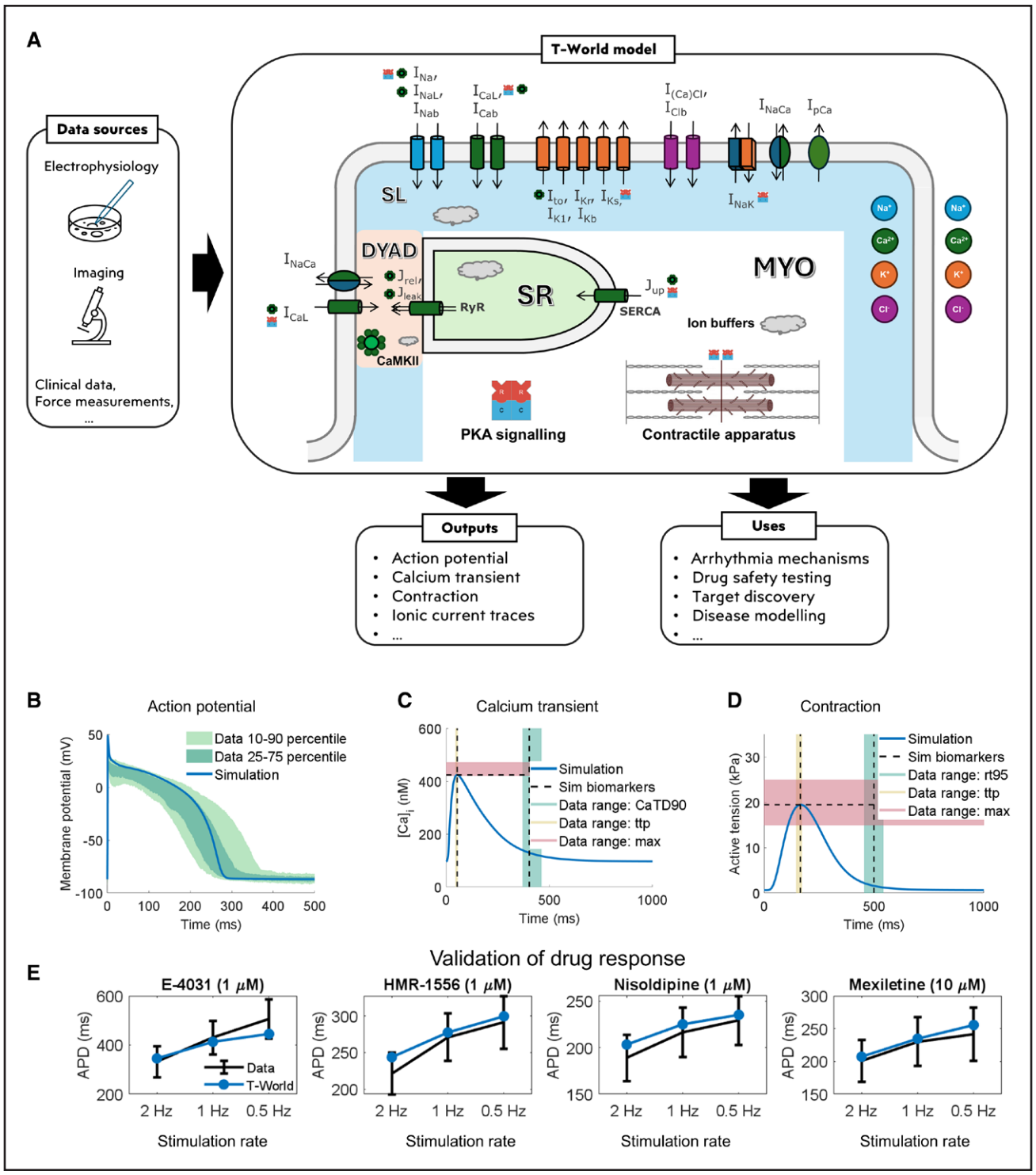

Figure 1. Model structure and key outputs.

A, Conceptual diagram of the T-World model and its potential applications. Model diagram shows the membrane with ionic currents (color-coded by ionic species). The inside of the cell is separated into the following compartments: DYAD (orange), subsarcolemmal (SL, blue), bulk myoplasm (MYO), and sarcoplasmic reticulum (SR, green). CaMKII (calcium/calmodulin-dependent protein kinase-II), and PKA (protein kinase-A) signaling pathways are included, with small icons adjacent to names of ionic currents, fluxes, or contractile apparatus indicating the site as a target of a given signaling pathway. Gray clouds indicate ionic buffers. **B**, Endocardial action potential (AP) of T-World vs experimental ranges.[18] A slightly higher peak membrane potential in simulation vs data was chosen, given that our model is a single cell, whereas the experimental data are in small tissue samples, which show a reduced peak due to cell-to-cell coupling. **C**, Calcium transient (CaT) of T-World with highlighted biomarkers vs experimental ranges for: CaT duration at 90% recovery level (CaTD90, shown in green), time to peak (ttp, shown in yellow), and CaT amplitude (shown as amplitude+diastolic level to facilitate comparison, in red), based on SE of mean ranges by Coppini et al.[19] **D**, Active tension developed by T-World with highlighted biomarkers vs experimental ranges for: time from peak to 95% recovery (rt95, shown in green), (*Continued*)

Downloaded from http://ahajournals.org by on April 7, 2026

recordings of simultaneous calcium and membrane potential changes.[31,32] However, T-World achieves this through physiologically realistic calcium-mediated calcium-induced calcium release. The Morotti2021 model also has calcium-mediated calcium-induced calcium release, but manifests an unrealistically slow initial CaT rise phase due to late SR release (Figure 2A). The TP06 model manifests a very large and early peaking CaT (Figure 2A), inconsistent with human data biomarkers, and order-of-magnitude too high dyadic calcium concentrations (Figure S8).

The biphasic CaT upstroke in Morotti2021 and its predecessors arises from SR release peaking around 30 to 40 ms, compared with the ≈10 to 15 ms peak seen in T-World, ToR-ORd, TP06 (Figure S9), and experimental data.[32–35] This delayed release not only slows early CaT rise but also affects the timing of calcium-dependent I_{CaL} inactivation, which should occur rapidly after calcium influx. Finally, late release generates depolarizing currents via NCX and $I_{(Ca)Cl}$ at 30 to 40 ms, distorting early AP morphology. Accelerating the SR release while retaining calcium sensitivity was therefore a major goal for T-World development.

Another major development target was the cell's response to changes in SERCA activity. Experimentally, SERCA activity is closely associated with CaT amplitude (Figure 2B), with SERCA potentiation increasing CaT amplitude and contractility,[36] and vice versa for reduced SERCA activity.[23,37] Capturing this relationship is key for simulating disease or sympathetic stimulation. The baseline Morotti2021 model and its predecessors show a limited agreement with data (Figure 2C and 2E), whereas the revised calcium-handling system in T-World provides good correspondence (Figure 2C and 2D).

In humans, CaT amplitude[24,25] and contraction force[24,26–29] rise with increasing stimulation frequency before declining at very high heart rates (Figure 2F through 2G), whereas SR calcium content increases monotonically in human[26] and rabbit[30] data (Figure 2H). T-World is in good agreement with these data, showing a nonmonotonic calcium- and force-frequency relationship, as well as a positive $[Ca]_{SR}$-frequency relationship (Figure 2I through 2K). This is nontrivial because the SR calcium load-release relationship is positive and steep in experiments[38] and computer models. The model, therefore, requires sufficient refractoriness of I_{CaL} and RyR to counterbalance this coupling at high pacing rates.

T-World's results quantitatively match several experimental data sets: peak $[Ca]_i$ rises to ≈150% of the 0.5 Hz level (Figure 2I and 2F), and developed force increases to ≈170%, closely matching human studies (Figure 2J and 2G). Other models show clear discrepancies: ToR-ORd exhibits, in steady state (Figure S10), a fully positive calcium–frequency relationship, while Morotti2021 shows a flat or negative calcium, force, and $[Ca]_{SR}$ rate-dependence at rates over 1 Hz, rather resembling a heart failure phenotype.[26,28] TP06 displays overly steep rate dependence and a biphasic SR calcium curve inconsistent with experiments (Figure S11).

I_{CaL} properties critically determine calcium handling. T-World manifests: (1) a data-like I_{CaL} current-voltage relationship (Figure S12A), which follows from (in)activation properties and maximum current amplitude, (2) a data-like recovery from refractoriness (substantially improving on ToR-ORd; Figure S12B), and (3) a good balance between voltage-dependent and calcium-dependent inactivation (Figure S12C and S12D).

Furthermore, calcium clearance during an AP is distributed as follows: SERCA 79.6%, NCX 20.15%, and sarcolemmal calcium pump 0.25%, in agreement with data from large mammals indicating SERCA dominance, 20% to 30% clearance by NCX, and pCa involvement.[39] Finally, further validation confirms that T-World reproduces the negative inotropic effects of sodium channel blockers and that sodium concentration changes with pacing rate qualitatively match experiments (Figure S13).

Sympathetic Nervous System Stimulation

Excitation-contraction coupling and electrophysiology are strongly modulated by the βAR signaling pathway, which mediates the myocardial response to sympathetic nervous stimulation. Our model includes the Heijman et al[40] βAR description, with modifications to account for updates to ionic currents and inclusion of the contractile apparatus in the model (Supplemental Methods). We calibrated T-World to achieve APD shortening with saturating activation of βARS, subsequently validating it by comparing the model outputs to human data on βARS-induced changes in CaT and contraction.

Activation of βARS in T-World causes a ≈7% APD shortening (Figure 3A), in line with human studies indicating APD shortening after isoproterenol exposure.[41,42] The elevation of early plateau potentials in the model, resulting from the increased I_{CaL}, was also consistent with data from canine cardiomyocytes exposed to isoproterenol.[43] βARS activation induces a large 2.68-fold increase in CaT amplitude (Figure 3B), consistent with

Figure 1 Continued. ttp (shown in yellow), and maximum active tension (max, shown in red), based on Margara et al.[20] **E**, Validation of the simulated AP duration (APD) in the presence of 1 μmol/L E-4031 (70% I_{Kr} block), 1 μmol/L HMR-1556 (90% I_{Ks} block), 1 μmol/L nisoldipine (90% L-type calcium channel [I_{CaL}] block), and 10 μmol/L mexiletine (54% I_{NaL}, 9% I_{Kr}, 20% I_{CaL} block) at 0.5, 1.0, and 2.0 Hz pacing using independent experimental data not used in model creation. Drug concentrations and their inhibitory effects on different currents are based on O'Hara et al.[18] Please note the distinct *y* axes for the 4 drugs. RyR indicates ryanodine receptor; and SERCA, sarco/endoplasmic reticulum Ca^{2+} ATPase.

Downloaded from http://ahajournals.org by on April 7, 2026

Circulation Research FIRST PROOF ONLY

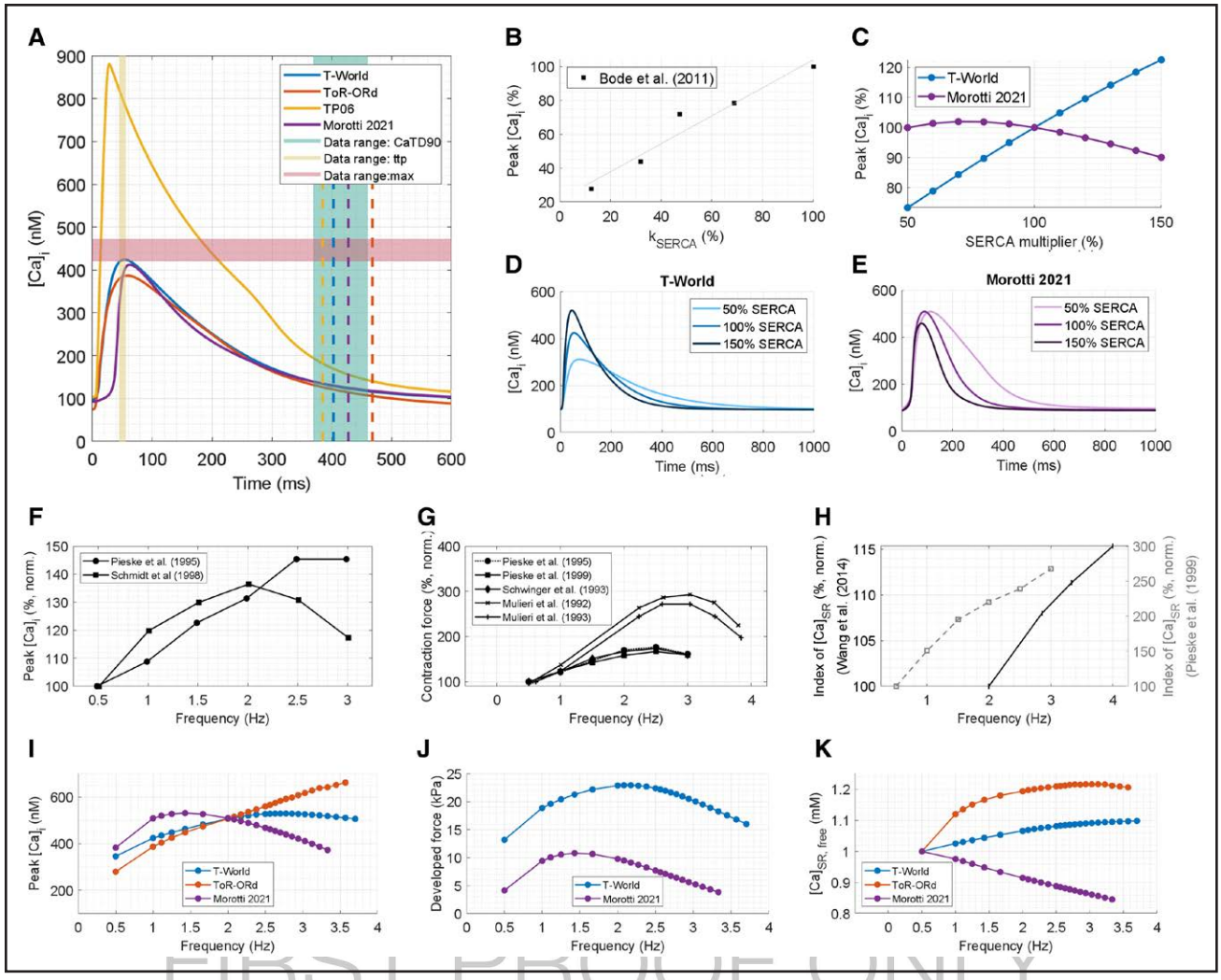

FIRST PROOF ONLY

Figure 2. Properties of excitation-contraction coupling.

A, Comparison of 4 models (T-World, ToR-ORd, Ten Tusscher-Panfilov 2006 model [TP06], and Morotti 2021) and experimental ranges for calcium-transient (CaT) properties; dashed lines give the CaT duration at 90% recovery for each model. **B** and **C**, Experimental data[23] (**B**) and model results (**C**) on the relationship between SERCA (sarco/endoplasmic reticulum Ca^{2+} ATPase) activity and peak calcium concentration. **D** and **E**, Sample traces of CaTs at 3 different SERCA levels. **F** through **H**, Experimental data for rate-dependence of peak calcium concentration,[24,25] developed force,[24,26–29] and sarcoplasmic reticulum (SR) calcium concentration.[26,30] In **H**, the Pieske et al[26] study in human samples used rapid cooling contractures, which is a less direct estimate of $[Ca]_{SR}$ than the direct measurement with a fluorescent dye by Wang et al[30] in rabbit. **I** through **K**, Corresponding simulations of rate-dependence in computational models. In **J**, only the models that include force generation are shown. The rate dependence of ToR-ORd depends on prepacing duration (Figure S10), whereas TP06 rate-dependence is very steep and is thus shown separately in Figure S11.

studies in humans and rabbits[44,45] that show a several-fold increase, although direct quantitative comparison is difficult, given the uncertain mapping of calcium-induced fluorescence changes to calcium concentrations. The 24% shortening of CaT at half-amplitude is similar to the ≈30% shortening observed in human samples.[45] Our model predicts a 2.63-fold increase in contractility (Figure 3C), which is generally in line with the highly heterogeneous human data that report an increase of 1.5-fold,[46] 3.0-fold, or 4.5-fold (depending on βARS-agonist[45]) and 5.0-fold.[47] Changes in kinetics of upstroke and recovery of contraction are also highly heterogeneous across different studies, although there is general agreement that βARS accelerates development and recovery of contraction,[45–47] as predicted by our model.

Similar predictions of substantially increased CaT amplitude and contraction are made by the Morotti2021 model, which also includes βARS, although APD does not shorten visibly in this model, and there is almost no plateau elevation (Figure S14).

Sex Differences

Pronounced differences exist between hearts from females and males, which subsequently translate into differential risk of various adverse cardiac outcomes.[48]

Downloaded from http://ahajournals.org by on April 7, 2026

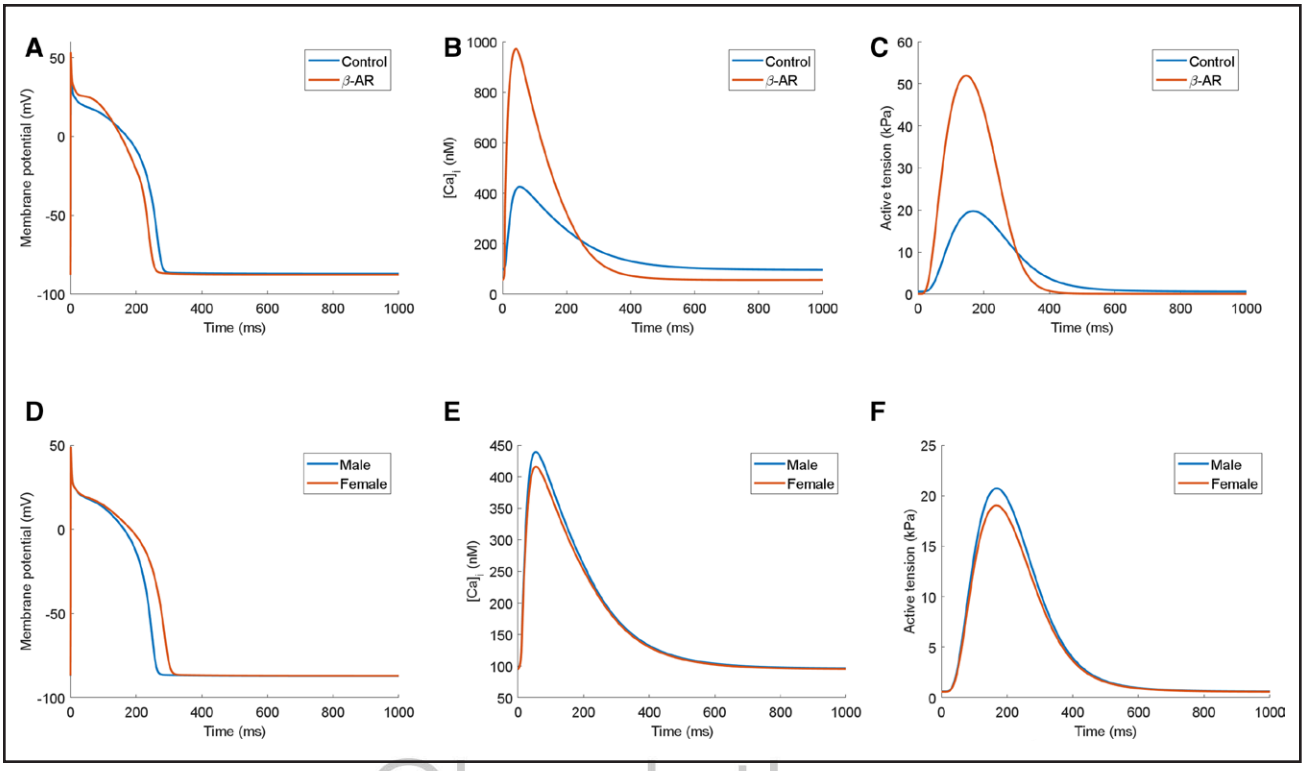

Figure 3. Effect of sympathetic nervous stimulation and sex differences in T-world.
A through **C**, Action potential, Ca^{2+}-transient, and contractility in the absence or presence of simulated βARS. **D** through **F**, Action potential, calcium transient, and contractility in male (blue) and female (orange) model versions. βAR indicates beta-adrenergic.

Circulation Research FIRST PROOF ONLY

Given the extent and importance of sex differences in cardiovascular physiology, we constructed a male and a female version of T-World, based on available experimental data and prior simulation approaches.[49–51] The female version of T-World has a prolonged APD (Figure 3D), and a slightly smaller CaT and peak developed force (Figure 3E and 3F), in agreement with available data.[52,53] Thus, sex-specific formulations of T-World correctly translate differences in ionic currents and buffering into key differences in overall phenotype, enabling studies into sex differences in arrhythmic risk (discussed below).

Cellular Arrhythmic Behaviors

There are 4 key arrhythmogenic behaviors at the cellular level: EADs, alternans, DADs, and steep restitution. Although previous models have been used to simulate subsets of these mechanisms, each of the available models recapitulates only a few mechanisms with (patho)physiologically relevant parameter values, indicating major limitations in the representation of underlying physiology and predictivity. As such, in-depth assessment of cellular arrhythmic behaviors represented a major focus of the present study.

Early Afterdepolarizations

EADs, extrasystolic depolarizations during an AP, contribute to arrhythmogenesis and are commonly linked to drug-induced cardiotoxicity and long QT syndromes, being typically driven by the reactivation of I_{CaL} during prolonged APD[13] (Figure 4A). T-World replicates EADs under realistic conditions of drug-induced long QT (Figure 4B), similar to ToR-ORd and ORd models,[4,18] with a 13-mV amplitude, similar to experimental observations.[54] At the same time, the good EAD-capability of T-World is not straightforward, given considerably greater and more data-like refractoriness of I_{CaL} compared with predecessors (Figure S12B). In contrast, the TP06 model requires nearly tripled I_{CaL} to manifest EADs,[56] likely due to excessive I_{Ks} providing strong repolarization reserve. The Morotti2021 model[11] similarly requires a 2.5-fold I_{CaL} to induce EADs (Figure S15).

T-World also highlights sex differences in EAD vulnerability. The female T-World variant requires less I_{Kr} inhibition to induce EADs compared with the male variant, indicating greater EAD vulnerability (Figure 4C), supporting data showing higher risk of drug-induced arrhythmia in female hearts.[49,57] In addition, female-specific apicobasal I_{CaL} gradients linked to estrogen[58] suggest an additional risk of EADs in basal regions of the heart in female models. In agreement, T-World shows increased EAD susceptibility in the female model version with increased I_{CaL} (Figure 4C).

Delayed Afterdepolarizations

DADs are arrhythmia triggers occurring during diastole. They result from spontaneous SR calcium release,

Downloaded from http://ahajournals.org by on April 7, 2026

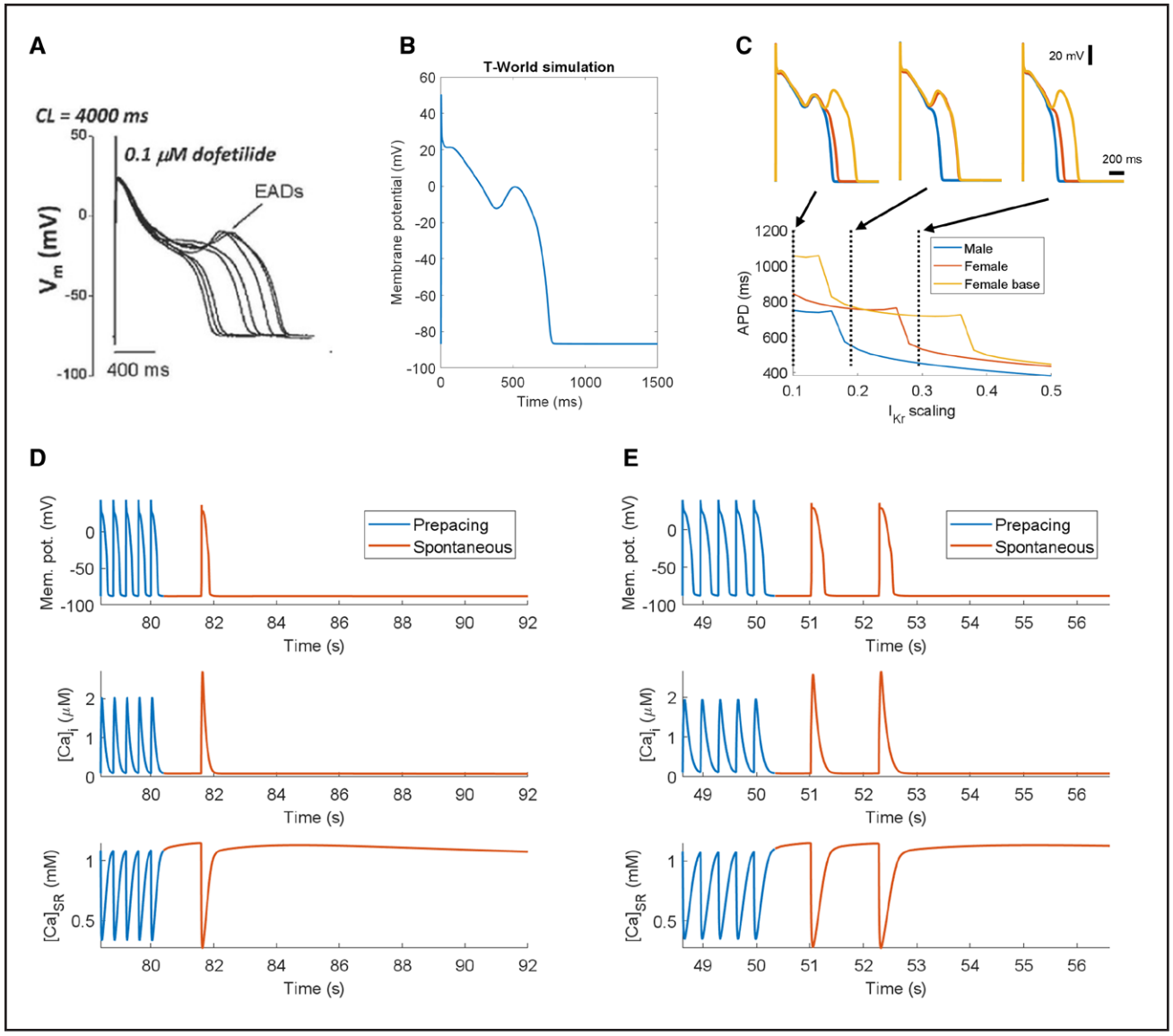

Figure 4. Early afterdepolarizations (EADs) and delayed afterdepolarizations (DADs) in T-World.
A and **B**, Experimental data (**A**) and model (**B**) showing EADs at 0.25 Hz pacing, with 85% block of I_{Kr} via dofetilide.[54] **C**, Demonstration of differential EAD formation under varying degrees of I_{Kr} availability in male and female model versions, as well as female+increased L-type calcium channel [I_{CaL}], reflecting the basal part of the female heart in a rabbit study.[55] The *y* axis shows action potential (AP) duration for a range of I_{Kr} scaling factors (fraction of current vs baseline) on the *x* axis, with sharp transitions corresponding to changes in the number of EADs. Insets show APs at corresponding dashed lines. **D**, Examples of triggered activity resulting from DADs (prepacing for 200 beats at 2.5 Hz, with fully active βAR (beta-adrenergic) signaling and extracellular calcium of 3.25 mmol/L). The end of the prepacing train is shown in blue, with the spontaneous activity given in red. **E**, Similar to **D** with 3 Hz, rather than 2.5 Hz prepacing rate for 150 beats, showing the generation of multiple triggered APs.

generating inward currents (primarily via NCX) that depolarize the cell[59] and are particularly prominent in diseased hearts, for example, in heart failure.[60] DADs arise from stochastic subcellular calcium sparks best simulated by models with spatial calcium handling and stochastic gating.[61] However, given the high computational cost of such models, common pool models with similar complexity as T-World, especially Bers/Grandi–like models, such as Morotti2021,[9–11] are often used to emulate DAD generation efficiently. By contrast, ToR-ORd cannot produce any DADs due to its RyR activation mechanism, whereas TP06 can yield DADs after parametric changes, but these differ substantially from experimental recordings.[62]

T-World manifests spontaneous calcium releases and DADs, and it can generate DAD trains, as observed in certain experiments[63] (Figure 4D and 4E). Spontaneous releases are terminated when the SR content becomes sufficiently low after the spontaneous releases, similar to simultaneous measurements of intracellular and SR calcium.[64] In this regard, our model differs from Morotti2021, where DADs stop occurring even when SR calcium keeps increasing (Figure S16).

Downloaded from http://ahajournals.org by on April 7, 2026

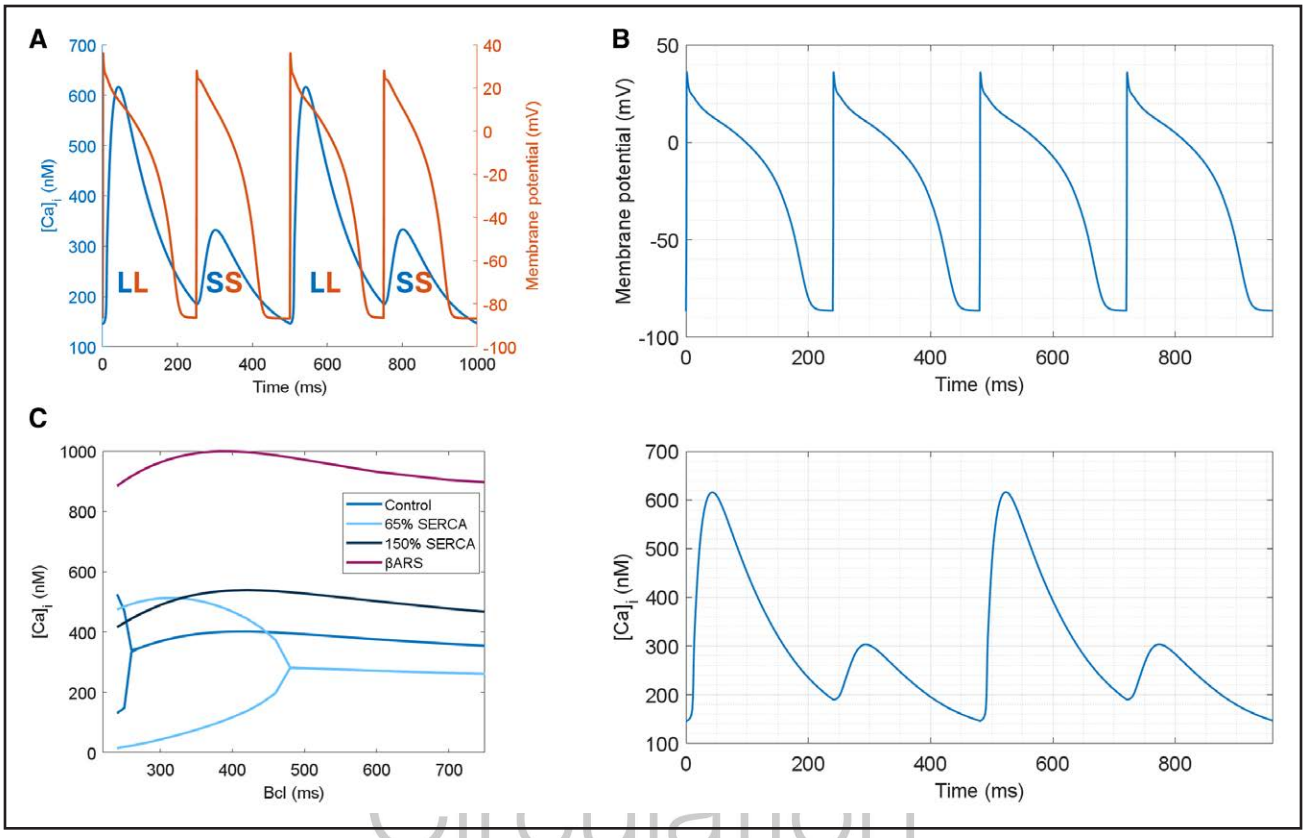

Figure 5. Alternans in T-World.
A, Illustration of concurrent oscillations in Ca^{2+} transient (blue) and action potential (AP) duration (orange). **B**, Calcium alternans in T-World under AP clamp based on a fixed-shape AP applied 250× at a basic cycle length of 240 ms. **C**, Modulation of calcium alternans by reduced or increased SERCA (sarco/endoplasmic reticulum Ca^{2+} ATPase) activity, as well as by βAR (beta-adrenergic) stimulation. LL indicates large/long calcium transient (CaT) and AP duration (APD), respectively; and SS, small/short.

Circulation Research
FIRST PROOF ONLY

To validate DADs in the model, we confirmed that faster prepacing and RyR sensitization promote DADs in T-World, as seen experimentally (Figure S17). Furthermore, for applications requiring stochasticity of DADs, we developed a version of T-World that includes stochastic store-overload-dependent RyR release akin to the method by Colman et al[65] (Figure S18).

Calcium and AP Alternans

Cardiac alternans, a periodic oscillation between long and short APDs, creates a proarrhythmic substrate, promoting conduction block[66] and increasing arrhythmia risk.[67] APD alternans is typically driven by underlying CaT oscillations and occurs at rapid heart rates.[68] Although common at high pacing rates in living hearts, many computer models do not recapitulate it, including the Bers/Grandi family, which provided the basis for the T-World calcium handling.

Thanks to its improved calcium handling, T-World produces AP and CaT alternans at realistic frequencies,[69] with mild alternans at 260 ms and pronounced alternans at 240 to 250 ms (Figure 5A; Figure S19). Alternans is electromechanically concordant (long APD corresponds to large CaT), matching experimental data in human-relevant species.[30,70,71] T-World shows CaT alternans even when a fixed AP shape is imposed, confirming calcium oscillations as the primary driver, rather than AP restitution (Figure 5B).

A major improvement of T-World compared with prior state-of-the-art is its correct response to alternans to SERCA pump changes. Consistent with conditions like heart failure and pharmacological or transcriptional SERCA reduction,[72–74] T-World shows increased alternans vulnerability with SERCA reduction, with alternans appearing at slower pacing rates (Figure 5C). This is in contrast with ToR-ORd, where SERCA inhibition suppresses alternans (Figure S20). Finally, we validated T-World by showing that an increase in SERCA function or βAR activation suppresses alternans (Figure 5C), in line with experimental data.[75,76]

Steep S1-S2 Restitution

Steep APD restitution (ie, a slope of the restitution curve >1) promotes arrhythmias by facilitating reentry and spiral wave breakup in cardiac tissue.[12,77] Human studies show that maximum curve slopes slightly above 1

Downloaded from http://ahajournals.org by on April 7, 2026

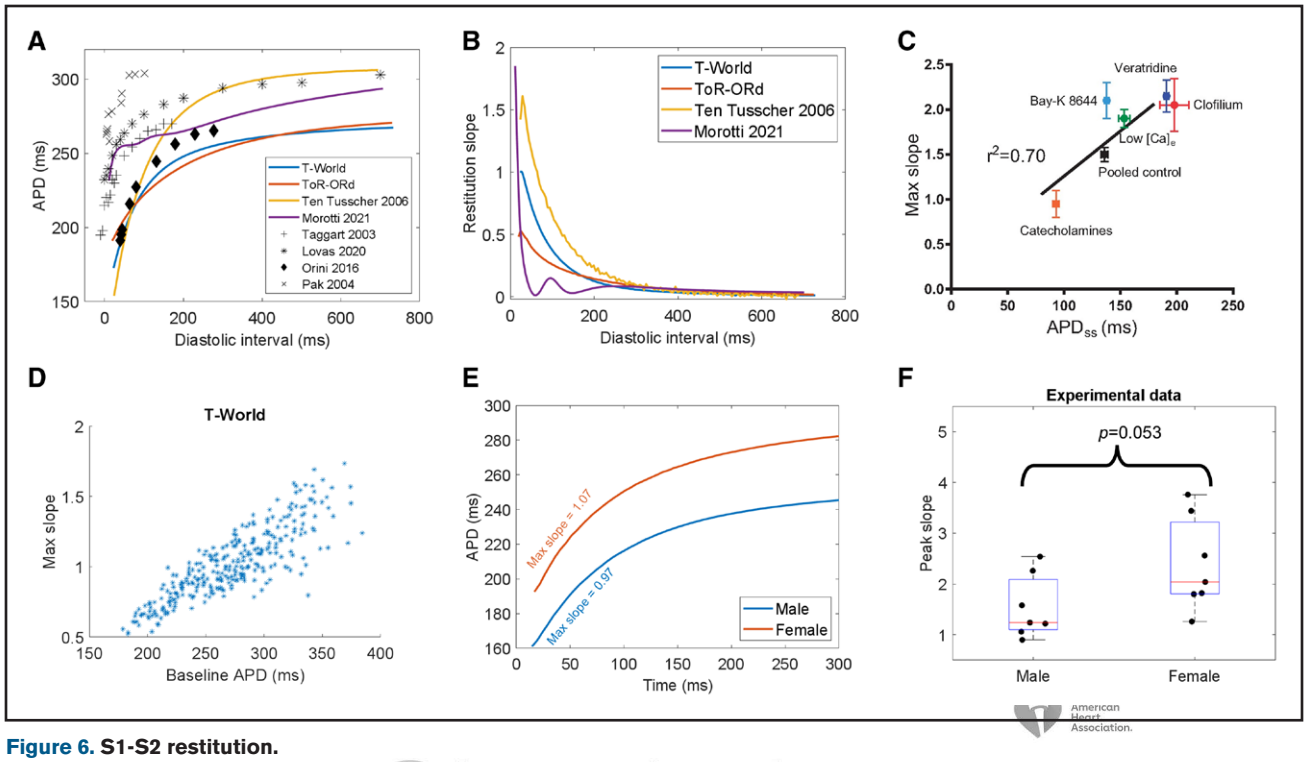

Figure 6. S1-S2 restitution.

A, S1-S2 restitution curve in the T-World, ToR-ORd, Morotti2021, and Ten Tusscher-Panfilov 2006 model (TP06) models, and a range of human studies.[78,80–82] **B**, Comparison of S1-S2 restitution slopes across T-World, ToR-ORd, Morotti2021, and TP06 models. **C**, Positive relationship between AP duration (APD) of a cell and its peak S1-S2 restitution slope, observed experimentally.[16] **D**, Corresponding simulation in T-World showing that when a range of ion channel conductances are varied (see Methods for details), cells with longer APD generally show a steeper slope of restitution. **E**, Steepening of restitution in female vs male myocytes in baseline T-World. **F**, Experimental human data comparing peak restitution slope in males vs females (n=7 in both groups, *P* value obtained using Mann-Whitney *U* test).

Circulation Research FIRST PROOF ONLY

are not uncommon.[78,79] The TP06 model has been historically popular because of its steep restitution properties, whereas, for example, the ToR-ORd model, on which most of T-World's electrophysiology is based, has a relatively flat restitution (peak slope ≈0.5). However, our revised I_{CaL} and other developments lead T-World to exhibit good agreement with experimental restitution data (Figure 6A), with an S1-S2 slope >1 for a subset of S2 intervals at an S1 interval of 1000 ms (Figure 6B). Restitution of APD is paralleled by the restitution of conduction velocity (Figure S21).

Shattock et al[16] have shown that the maximum slope of the restitution curve is largely determined by the steady-state APD of a cell. Specifically, the longer the APD, the steeper the restitution (Figure 6C), which was corroborated by multiple experimental studies using different means of changing APD.[83–85] Importantly, T-World is the only model among those capable of steep restitution that recapitulates this feature (Figure 6D), with the TP06 model showing a weakly inverse APD-slope relationship, and the Morotti2021 a strongly inverse one (Figure S22). This makes T-World uniquely suitable for studying how APD changes due to disease or drugs modulating arrhythmic risk via restitution changes.

One notable exception to the observation by Shattock et al[16] is the effect of βAR stimulation, which shortens APD but steepens the S1-S2 slope in humans.[78] As an independent validation, we simulated the effect of βAR activation in the T-World model, which produced the correct phenotype (Figure S23). Furthermore, we validated that shortening of the S1 interval indeed flattens the S1-S2 restitution (Figure S24).

Measuring restitution slope separately for the male and female versions of T-World, we observed a steeper slope in the female myocyte (Figure 6E; Figure S25). This would point to an increased risk of arrhythmia in female hearts through steeper restitution, but intriguingly, we were unable to find any experimental study addressing this hypothesis. However, we were able to obtain human ventricular data from the study by Árpádffy-Lovas et al[80] and reanalyzed them for sex differences in peak slope. Mean (SD) peak slope in males was 1.54 (±0.63), increasing to a mean of 2.38 (±0.92) in females (*P*=0.053, Mann-Whitney *U* test, Figure 6F). This suggests that females may have steeper restitution properties, a previously underappreciated sex-specific hazard.

Stability of Arrhythmic Behaviors

To validate the generality and robustness of T-World, we investigated the stability of the cellular arrhythmic

Downloaded from http://ahajournals.org by on April 7, 2026

behaviors under parameter perturbation using a population-of-models approach with key ionic currents and fluxes varied between 67% and 150%. Although it is natural for cells, living and simulated alike, to manifest arrhythmogenic behaviors under slightly different conditions, the majority of cells should be fundamentally capable of manifesting them. Overall, 786 out of 1000 models passed all the calibration criteria derived from human data (Supplemental Methods for details) and were used subsequently. In total, 99.5% of the 786 models manifest EADs for a sufficient I_{Kr} and I_{CaL} perturbation, while 88% manifest DADs for a sufficiently high extracellular calcium, increasing to 93.4% when increasing SERCA by 50% to facilitate SR calcium overload (Figure 7A and 7B). The key factor preventing DADs in a part of the population is increased I_{NaCa} (Figure S26) because this can clear released calcium more rapidly from the dyadic space, which limits the pro-DAD condition of high dyadic calcium combined with high $[Ca]_{SR}$ load, as also observed previously.[86] In total, 708 models in the population can capture all stimuli at a cycle length of 260 ms, and 99% of these manifest alternans for at least 1 tested SERCA multiplier (Figure S7C). Finally, 48.5% of models exhibit a restitution slope > 1 (Figure 7D), consistent with 44%,[79] 74%,[87] and 61%.[81] of samples in human recordings. Thus, T-World is highly robust with regard to its arrhythmia precursor capabilities, which are its intrinsic properties, rather than phenomena that only occur for highly specific sets of distinct parameters for each property. This is a fundamental advance compared with prior major models, which show a limited range of arrhythmogenic behaviors, and often with major caveats (Figure 7E).

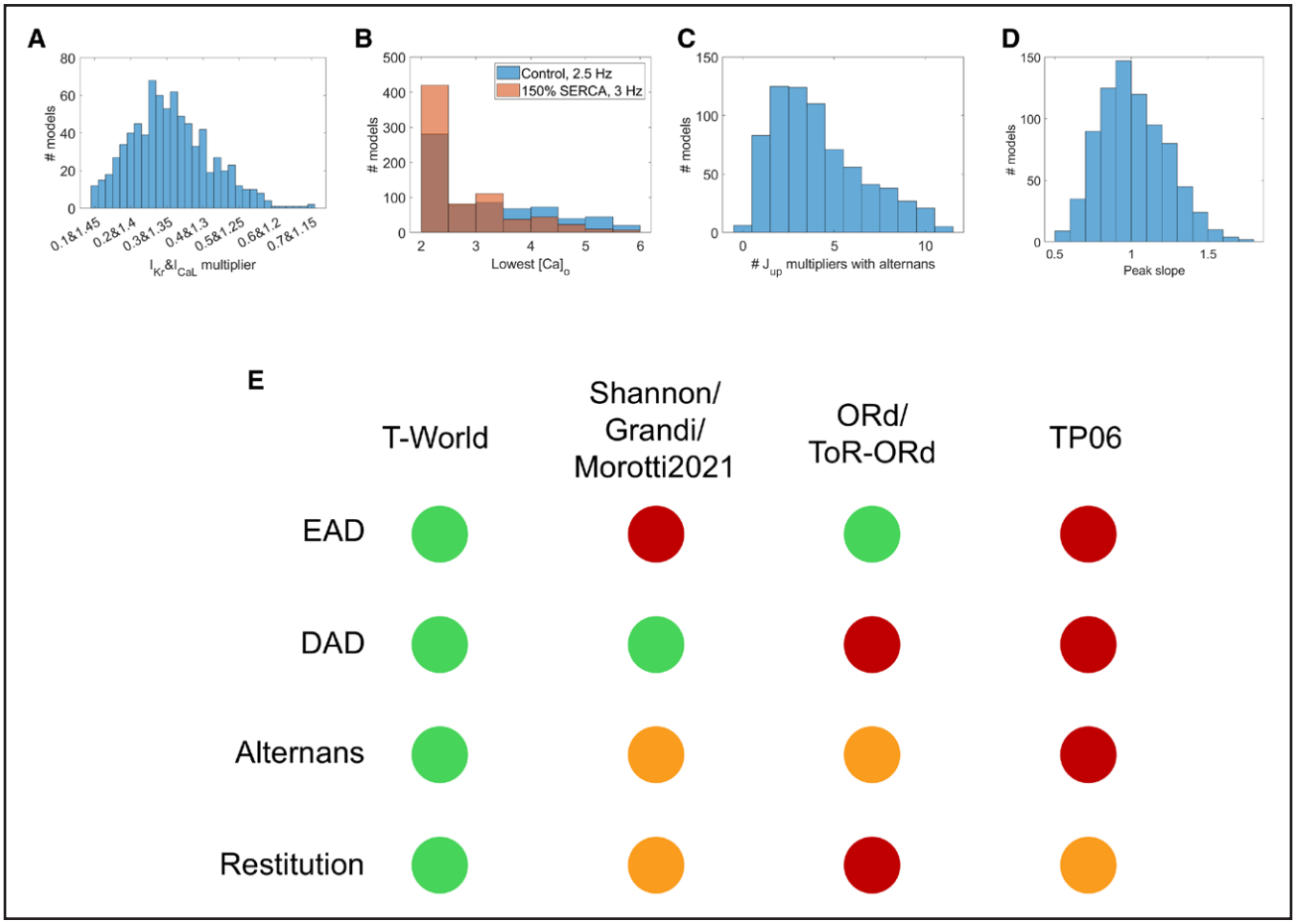

Figure 7. Stability of arrhythmic behaviors in T-World.
A, Histogram describing the degree of proearly afterdepolarization (EAD) alteration to the baseline cell (increasing L-type calcium channel [I_{CaL}] and reducing I_{Kr}) that is sufficient to trigger EADs in each model in a calibrated population of models (see Arrhythmia Studies in Supplemental Methods for details). **B**, Histogram of the level of extracellular calcium that is sufficient to trigger delayed afterdepolarizations (DADs) after rapid prepacing in the presence of βARS stimulation in the baseline T-World model and a version with 50% higher SERCA (sarco/endoplasmic reticulum Ca^{2+} ATPase) activity. **C**, Histogram showing how many models among those with J_{up} multipliers of 0.5, 0.6, …, 1.5 (11 in total) manifest alternans at 260 ms basic cycle length. **D**, Distribution of peak S1-S2 slopes in the calibrated population. **E**, Visual comparison of T-World and prior modeling families, depicting whether an arrhythmogenic behavior is stable and satisfactory (green), present in principle with caveats (eg, requiring substantial parameter changes or via unphysiological mechanisms; orange), or almost completely or completely absent (red). See Figure S27 for further details on simulations and criteria underlying the diagram.

Downloaded from http://ahajournals.org by on April 7, 2026

DISCUSSION

We developed, calibrated, and validated T-World, a new computer model of the human ventricular cardiomyocyte designed to meet the longstanding need for a highly general human-specific virtual cardiac cell. Integrating innovations with carefully curated elements from the Rudy-like[4,18] and Grandi and Bers[9,10] models, T-World unifies these 2 major model families, combining their strengths while resolving key limitations. Unlike predecessor models with limited arrhythmogenic capabilities, it reproduces, in a single model, the generation of EADs and DADs, realistic restitution dynamics, and calcium-driven alternans responsive to SERCA modulation.

The model's credibility is supported by extensive calibration to human data (Table S1), independent validation on unseen data (Table S2), and construction from well-characterized components. Unlike machine learning models with billions of free parameters, T-World is built from components (ionic channels and signaling pathways), which were derived from experimental measurements, markedly reducing the risk of model overfitting and consequent incorrect predictions. Its universality and adaptability make it valuable for basic research, drug testing, and patient-specific virtual twins.[88]

T-World advances the 3Rs principles: particularly reduction and (partial) replacement of animal use. It is synergistic with in vitro systems such as induced pluripotent stem cell–derived cardiomyocytes, helping interpret their immature phenotypes in an adult-heart context. Its human-specificity also enables the translation of animal data, such as protein-level changes, into predictions of functional implications for human physiology. There are important differences between the hearts of humans and animals, particularly the most popular experimental animal models such as mice and rats.[89] For example, most episodes of drug-induced arrhythmia in humans are due to drug-induced inhibition of hERG channels,[90] but this channel is nearly absent in the hearts of mice and rats. As such, testing the safety of drugs in those species is of limited use, as those species lack the key component responsible for the issue. We note that in this context, human specificity refers predominantly to the phenotype produced and focuses on using human data in calibration and validation. Although the model utilizes human data to describe the kinetics of ionic channels and other processes wherever possible, some model components are based on prior animal-based formulations, as human data are absent.

T-World represents sex differences in cardiac cell physiology, and its simulations, supported by newly analyzed human data, suggest that females may be more prone to steep restitution slopes. This is in addition to higher EAD susceptibility observed here and previously,[49,57] with both mechanisms promoting arrhythmia at the tissue level.[12,77] The finding of likely steeper restitution in females highlights T-World's potential to generate biological insights but warrants confirmation in larger studies. The results reinforce the need for sex-specific drug dosing and treatment guidelines, which remain insufficiently addressed.[91]

T-World's strong calcium handling and excitation-contraction coupling make it well-suited for diseases with pronounced calcium remodeling, such as heart failure and postinfarction remodeling. Unlike models like ToR-ORd, T-World can produce DADs, important in such diseases.[60] A particular strength pertaining to arrhythmia mechanisms is that T-World exhibits increased alternans vulnerability with a reduction in SERCA activity, both hallmarks of those diseases. This is an improvement over major prior human models such as ORd and ToR-ORd,[4,18] which do not respond well to SERCA changes, and are thus less suitable for modeling this aspect of disease.

Incorporation of βAR signaling and excitation-contraction coupling modulation makes T-World particularly useful for studies of the neurocardiac axis and sympathetic control of arrhythmia.[92] Validation results demonstrate strong predictive performance for multiple arrhythmic mechanisms influenced by sympathetic activation, underscoring its utility for mechanistic and translational research. As more data become available on electrophysiological and signaling effects of sympathetic neurotransmitters such as Neuropeptide Y, it will be interesting to incorporate these, given their proarrhythmic role.[93] Incorporation of parasympathetic signaling is another likely direction of development.

The main limitation of computer models like T-World is that they can only reproduce behaviors that emerge from the components explicitly included. Yet this limitation can serve as a powerful research tool. When a model's predictions diverge from experimental observations, the discrepancy can highlight gaps in our biological understanding, pointing, for example, to a missing signaling pathway that may contribute to the observed phenomenon. Such omissions might explain, for instance, the lack of APD shortening in response to elevated extracellular calcium in T-World (Supplemental Note 1).

A known limitation of models at this level of abstraction is their inability to accurately represent DAD origins and the spatial heterogeneity of subcellular calcium handling. DADs arise from localized spontaneous calcium releases that spread diffusively through the cell, recruiting additional RyRs. Because T-World and similar models describe only average calcium concentrations per compartment, they cannot capture this within-compartment diffusion process. Likewise, it is challenging to represent certain changes in subcellular structure, such as changes in T-tubule density or dispersion of RyRs, important, for example, in heart failure.[94] Spatially distributed models, which represent thousands of RyR and I_{CaL}, clusters can simulate calcium wave propagation and T-tubule structure more realistically[95] and can provide more detailed insights into the subcellular determinants of calcium-driven alternans that are present

Circulation Research FIRST PROOF ONLY

Downloaded from http://ahajournals.org by on April 7, 2026

at a whole-cell scale in T-World.[96] At the same time, they are computationally demanding (up to an hour per beat, as opposed to ≈0.15s in T-World) and less scalable, occupying a different niche with regard to applications. This makes developing hybrid approaches that incorporate spatial diffusion into T-World–like frameworks an interesting direction for future research.

On the other end of the model complexity spectrum, while T-World is suitable for 3-dimensional organ-scale simulations (as demonstrated in the second article), considerably simpler models may enable more high-throughput studies focused on conduction properties, where cellular realism is not a priority. Such models include, for example, the TP06 model also investigated here,[12] or the even simpler and more computationally efficient minimal ventricular model by Bueno-Orovio et al.[97]

The versatility and broad applicability of T-World open new avenues in cardiac research and predispose it to further extensions, such as variants representing disease remodeling, channel mutations, or investigating nonstandard ionic channels. We envision that its universality, modularity, and open-source nature will also enable adaptations to represent other excitable cells, such as atrial, sinoatrial, Purkinje, or neuronal. It will also facilitate studies on newly discovered ionic currents, and on understanding signaling pathways and how they modulate cellular physiology. To expand the model's generality, we anticipate it will be particularly important to represent dynamic regulation of trafficking and transcription,[98] enabling studies on long-term remodeling, representation of mitochondria, metabolism, and reactive oxygen species,[99] integration with AI-driven structural modeling,[100] and omics analyses.[101]

To support continued development while preserving reproducibility, we will treat T-World as a versioned, openly released framework. Incremental extensions (eg, adding a mutation or a narrowly targeted remodeling mechanism) can typically be implemented modularly without affecting baseline behavior, whereas more disruptive changes to central subsystems (eg, calcium handling) will warrant revalidation using the same calibration and validation criteria established here. Each public release will be assigned a distinct version number (current: v1.0) and accompanied by a transparent changelog and archived code snapshot, enabling users to reproduce published results and to identify precisely what changed between versions. Importantly, future refinements will be evaluated against the current model's defining behaviors and predictive benchmarks; any trade-offs introduced by extensions will therefore be detected explicitly and reported, ensuring that improvements do not inadvertently compromise the capabilities demonstrated in this article.

ARTICLE INFORMATION

Received December 16, 2025; revision received March 12, 2026; accepted March 19, 2026.

Affiliations

Department of Anatomy, Physiology and Genetics (J.T., H.J.), Department of Computer Science (M.H., A.B., A.B.-O., B.R.), and Ludwig Cancer Research (M.T.), University of Oxford, United Kingdom. Department of Pharmacology, University of California, Davis (J.T., D.M.B.). Department of Physiology, McGill University, Montreal, CA (T.B.). Department of Pharmacology and Pharmacotherapy, University of Szeged, Hungary (N.N.). School of Biomedical Sciences, University of Leeds, United Kingdom (M.A.C.). Division of Medical Physics and Biophysics, Gottfried Schatz Research Center, Medical University of Graz, Austria (J.H.). Cardiovascular Research Institute Maastricht (CARIM), Faculty of Health, Medicine and Life Sciences, Maastricht University, the Netherlands (J.H.).

Acknowledgments

The authors thank Eleonora Grandi, Stefano Morotti, and Haibo Ni for useful discussions on how models derived from Shannon et al operate. The authors also thank Dirk Gillespie, Dezso Boda, Pavel Jungwirth, and Geir Halnes for their insights on how ionic driving force through open L-type calcium channels should or should not be modeled, and Roshni Shetty and David Ortega for spotting minor issues in the code.

For the purpose of open access, the authors have applied a Creative Commons Attribution (CC-BY-NC) public copyright license to any Author Accepted Manuscript version arising from this submission.

Author Contributions

J. Tomek conceptualized and coordinated the study, designed, developed, and validated the model with contributions from J. Heijman, D.M. Bers, M.A. Colman, and A. Bueno-Orovio. J. Heijman, D.M. Bers, and B. Rodriguez jointly supervised the project. J. Tomek and J. Heijman wrote the initial draft, subsequently revised by D.M. Bers, B. Rodriguez, M. Tomkova, A. Bertrand, M.A. Colman, and A. Bueno-Orovio. M. Holmes developed the formulation of sex differences and performed conduction velocity restitution simulations. T. Bury developed the online application to run T-World. M. Tomkova contributed to genetic algorithm fitness design, visualization, and modeling design choices. H. Jo generated codes to assess sodium-potassium pump function and contributed to its redesign. N. Nagy provided and analyzed experimental data on sex differences in S1-S2 restitution.

Sources of Funding

J. Tomek is supported by the Sir Henry Wellcome Fellowship (222781/Z/21/Z). J. Heijman was supported by the Netherlands Heart Foundation (grant no. 01-002-2022-0118, EmbRACE: Electro-Molecular Basis and the Therapeutic Management of Atrial Cardiomyopathy, Fibrillation and Associated Outcomes) and the Netherlands Organization for Scientific Research (NWO/ZonMW Vidi 09150171910029). D. Bers is supported by National Institutes of Health grants P01-HL141084 and R01-HL092097. This work was also supported by a Wellcome Trust Fellowship in Basic Biomedical Sciences to B. Rodriguez (214290/Z/18/Z) and the CompBioMedX project (to B. Rodriguez, EP/X019446/1). The project was further supported by the National Research, Development, and Innovation Office (NKFIH FK-142949 for N. Nagy). H. Jo is funded by the BBSRC's Interdisciplinary Bioscience DTP. T. Bury is supported by a Fonds de Recherche du Québec—Nature et Technologies (FRQNT) postdoctoral fellowship. A. Bertrand is supported by EPSRC Centre for Doctoral Training in Health Data Science scholarship (EP/S02428X/1) and the EPSRC Postdoctoral Pathway Fellowship (EP/Z534870/1). A Bueno-Orovio acknowledges support from the Innovate UK grant 10110728. M.A. Colman is supported by a Medical Research Council Career Development Award (grant no. MR/V010050/1).

Disclosures

None.

Supplemental Material

Supplemental Methods
Tables S1–S6
Figures S1–S27
Major Resources Table
References 74,102–167

REFERENCES

1. Trayanova NA, Lyon A, Shade J, Heijman J. Computational modeling of cardiac electrophysiology and arrhythmogenesis: toward clinical translation. *Physiol Rev.* 2024;104:1265–1333. doi: 10.1152/physrev.00017.2023
2. Boyle PM, Zghaib T, Zahid S, Ali RL, Deng D, Franceschi WH, Hakim JB, Murphy MJ, Prakosa A, Zimmerman SL, et al. Computationally guided

Circulation Research FIRST PROOF ONLY

Downloaded from http://ahajournals.org by on April 7, 2026

personalized targeted ablation of persistent atrial fibrillation. *Nat Biomed Eng*. 2019;3:870–879. doi: 10.1038/s41551-019-0437-9
3. Passini E, Britton OJ, Lu HR, Rohrbacher J, Hermans AN, Gallacher DJ, Greig RJH, Bueno-Orovio A, Rodriguez B. Human in silico drug trials demonstrate higher accuracy than animal models in predicting clinical pro-arrhythmic cardiotoxicity. *Front Physiol*. 2017;8:668. doi: 10.3389/fphys.2017.00668
4. Tomek J, Bueno-Orovio A, Passini E, Zhou X, Minchole A, Britton O, Bartolucci C, Severi S, Shrier A, Virag L, et al. Development, calibration, and validation of a novel human ventricular myocyte model in health, disease, and drug block. *Elife*. 2019;8:e48890. doi: 10.7554/eLife.48890
5. Varró A, Tomek J, Nagy N, Virág L, Passini E, Rodriguez B, Baczkó I. Cardiac transmembrane ion channels and action potentials: cellular physiology and arrhythmogenic behavior. *Physiol Rev*. 2021;101:1083–1176. doi: 10.1152/physrev.00024.2019
6. UK Government policy paper: replacing animals in science: a strategy to support the development, validation and uptake of alternative methods. 2025.
7. Food and Drug Administration. Roadmap to reducing animal testing in preclinical safety studies. 2025
8. European Medicines Agency. EMA regulatory science to 2025 strategic reflection. 2025
9. Shannon TR, Wang F, Puglisi J, Weber C, Bers DM. A mathematical treatment of integrated Ca dynamics within the ventricular myocyte. *Biophys J*. 2004;87:3351–3371. doi: 10.1529/biophysj.104.047449
10. Grandi E, Pasqualini FS, Bers DM. A novel computational model of the human ventricular action potential and Ca transient. *J Mol Cell Cardiol*. 2010;48:112–121. doi: 10.1016/j.yjmcc.2009.09.019
11. Morotti S, Liu C, Hegyi B, Ni H, Iseppe AF, Wang L, Pritoni M, Ripplinger CM, Bers DM, Edwards AG, et al. Quantitative cross-species translators of cardiac myocyte electrophysiology: model training, experimental validation, and applications. *Sci Adv*. 2021;7:927. doi: 10.1126/sciadv.abg0927
12. Tusscher KHWJ, Panfilov AV. Alternans and spiral breakup in a human ventricular tissue model. *Am J Physiol Heart Circ Physiol*. 2006;291:H1088–H1100. doi: 10.1152/ajpheart.00109.2006
13. Weiss JN, Garfinkel A, Karagueuzian HS, Chen PS, Qu Z. Early afterdepolarizations and cardiac arrhythmias. *Heart Rhythm*. 2010;7:1891–1899. doi: 10.1016/j.hrthm.2010.09.017
14. Liu MB, De Lange E, Garfinkel A, Weiss JN, Qu Z. Delayed afterdepolarizations generate both triggers and a vulnerable substrate promoting reentry in cardiac tissue. *Heart Rhythm*. 2015;12:2115–2124. doi: 10.1016/j.hrthm.2015.06.019
15. Edwards JN, Blatter LA. Cardiac alternans and intracellular calcium cycling. *Clin Exp Pharmacol Physiol*. 2014;41:524–532. doi: 10.1111/1440-1681.12231
16. Shattock MJ, Park KC, Yang HY, Lee AWC, Niederer S, MacLeod KT, Winter J. Restitution slope is principally determined by steady-state action potential duration. *Cardiovasc Res*. 2017;113:817–828. doi: 10.1093/cvr/cvx063
17. Tomek J, Holmes M, Martinez-Navarro H, Zhou X, Hasaballa AI, Wang ZJ, Arantes Berg L, Bertrand A, Colman MA, Bueno-Orovio A, et al. T-world: a highly general in silico human ventricular cardiomyocyte. II. Organ-scale simulations and applications. *Circ Res*. 2025
18. O'Hara T, Virág L, Varró A, Rudy Y. Simulation of the undiseased human cardiac ventricular action potential: model formulation and experimental validation. *PLoS Comput Biol*. 2011;7:e1002061. doi: 10.1371/journal.pcbi.1002061
19. Coppini R, Ferrantini C, Yao L, Fan P, Del Lungo M, Stillitano F, Sartiani L, Tosi B, Suffredini S, Tesi C, et al. Late sodium current inhibition reverses electromechanical dysfunction in human hypertrophic cardiomyopathy. *Circulation*. 2013;127:575–584. doi: 10.1161/CIRCULATIONAHA.112.134932
20. Margara F, Wang ZJ, Levrero-Florencio F, Santiago A, Vázquez M, Bueno-Orovio A, Rodriguez B. In-silico human electro-mechanical ventricular modelling and simulation for drug-induced pro-arrhythmia and inotropic risk assessment. *Prog Biophys Mol Biol*. 2021;159:58–74. doi: 10.1016/j.pbiomolbio.2020.06.007
21. Land S, Park-Holohan SJ, Smith NP, dos Remedios CG, Kentish JC, Niederer SA. A model of cardiac contraction based on novel measurements of tension development in human cardiomyocytes. *J Mol Cell Cardiol*. 2017;106:68–83. doi: 10.1016/j.yjmcc.2017.03.008
22. Weiss JN, Karma A, MacLellan WR, Deng M, Rau CD, Rees CM, Wang J, Wisniewski N, Eskin E, Horvath S, et al. "Good enough solutions" and the genetics of complex diseases. *Circ Res*. 2012;111:493–504. doi: 10.1161/CIRCRESAHA.112.269084
23. Bode EF, Briston SJ, Overend CL, O'Neill SC, Trafford AW, Eisner DA. Changes of SERCA activity have only modest effects on sarcoplasmic reticulum Ca^{2+} content in rat ventricular myocytes. *J Physiol*. 2011;589:4723–4729. doi: 10.1113/jphysiol.2011.211052
24. Pieske B, Kretschmann B, Meyer M, Holubarsch C, Weirich J, Posival H, Minami K, Just H, Hasenfuss G. Alterations in intracellular calcium handling associated with the inverse force-frequency relation in human dilated cardiomyopathy. *Circulation*. 1995;92:1169–1178. doi: 10.1161/01.cir.92.5.1169
25. Schmidt U, Hajjar RJ, Helm PA, Kim CS, Doye AA, Gwathmey JK. Contribution of abnormal sarcoplasmic reticulum ATPase activity to systolic and diastolic dysfunction in human heart failure. *J Mol Cell Cardiol*. 1998;30:1929–1937. doi: 10.1006/jmcc.1998.0748
26. Pieske B, Maier LS, Bers DM, Hasenfuss G. Ca2+ handling and sarcoplasmic reticulum Ca2+ content in isolated failing and nonfailing human myocardium. *Circ Res*. 1999;85:38–46. doi: 10.1161/01.res.85.1.38
27. Schwinger RHG, Böhm M, Koch A, Uhlmann R, Überfuhr P, Kreuzer E, Reichart B, Erdmann E. Force-frequency-relation in human atrial and ventricular myocardium. *Mol Cell Biochem*. 1993;119:73–78. doi: 10.1007/BF00926856
28. Mulieri LA, Hasenfuss G, Leavitt B, Allen PD, Alpert NR. Altered myocardial force-frequency relation in human heart failure. *Circulation*. 1992;85:1743–1750. doi: 10.1161/01.cir.85.5.1743
29. Mulieri LA, Leavitt BJ, Martin BJ, Haeberle JR, Alpert NR. Myocardial force-frequency defect in mitral regurgitation heart failure is reversed by forskolin. *Circulation*. 1993;88:2700–2704. doi: 10.1161/01.cir.88.6.2700
30. Wang L, Myles RC, De Jesus NM, Ohlendorf AKP, Bers DM, Ripplinger CM. Optical Mapping of sarcoplasmic reticulum Ca^{2+} in the intact heart: ryanodine receptor refractoriness during alternans and fibrillation. *Circ Res*. 2014;114:1410–1421. doi: 10.1161/CIRCRESAHA.114.302505
31. Choi BR, Salama G. Simultaneous maps of optical action potentials and calcium transients in guinea-pig hearts: mechanisms underlying concordant alternans. *J Physiol*. 2000;529 Pt 1:171–188. doi: 10.1111/j.1469-7793.2000.00171.x
32. Shkryl VM, Blatter LA. Ca^{2+} release events in cardiac myocytes up close: insights from fast confocal imaging. *PLoS One*. 2013;8:e61525. doi: 10.1371/journal.pone.0061525
33. Shannon TR, Ginsburg KS, Bers DM. Potentiation of fractional sarcoplasmic reticulum calcium release by total and free intra-sarcoplasmic reticulum calcium concentration. *Biophys J*. 2000;78:334–343. doi: 10.1016/S0006-3495(00)76596-9
34. Novotová M, Zahradníková A, Nichtová Z, Kováč R, Kráľová E, Stankovičová T, Zahradníková A, Zahradník I. Structural variability of dyads relates to calcium release in rat ventricular myocytes. *Sci Rep*. 2020;10:8076. doi: 10.1038/s41598-020-64840-5
35. Puglisi JL, Yuan W, Bassani JW, Bers DM. Ca^{2+} influx through Ca^{2+} channels in rabbit ventricular myocytes during action potential clamp: influence of temperature. *Circ Res*. 1999;85:e7–e16. doi: 10.1161/01.res.85.6.e7
36. Baker DL, Hashimoto K, Grupp IL, Ji Y, Reed T, Loukianov E, Grupp G, Bhagwhat A, Hoit B, Walsh R, et al. Targeted overexpression of the sarcoplasmic reticulum Ca^{2+}-ATPase increases cardiac contractility in transgenic mouse hearts. *Circ Res*. 1998;83:1205–1214. doi: 10.1161/01.res.83.12.1205
37. Hasenfuss G, Reinecke H, Studer R, Pieske B, Meyer M, Drexler H, Just H. Calcium cycling proteins and force-frequency relationship in heart failure. *Basic Res Cardiol*. 1996;91:17–22. doi: 10.1007/BF00795357
38. Shannon TR, Ginsburg KS, Bers DM. Quantitative assessment of the SR Ca^{2+} leak-load relationship. *Circ Res*. 2002;91:594–600. doi: 10.1161/01.res.0000036914.12686.28
39. Bers DM. *Excitation-Contraction Coupling and Cardiac Contractile Force*. Kluwer Academic Publishers; 2001.
40. Heijman J, Volders PGA, Westra RL, Rudy Y. Local control of β-adrenergic stimulation: effects on ventricular myocyte electrophysiology and Ca^{2+}-transient. *J Mol Cell Cardiol*. 2011;50:863–871. doi: 10.1016/j.yjmcc.2011.02.007
41. Lang D, Holzem K, Kang C, Xiao M, Hwang HJ, Ewald GA, Yamada KA, Efimov IR. Arrhythmogenic remodeling of β2 versus β1 adrenergic signaling in the human failing heart. *Circ Arrhythm Electrophysiol*. 2015;8:409–419. doi: 10.1161/CIRCEP.114.002065
42. Shimizu W, Ohe T, Kurita T, Takaki H, Aihara N, Kamakura S, Matsuhisa M, Shimomura K. Early afterdepolarizations induced by isoproterenol in patients with congenital long QT syndrome. *Circulation*. 1991;84:1915–1923. doi: 10.1161/01.cir.84.5.1915
43. Szentandrássy N, Farkas V, Bárándi L, Hegyi B, Ruzsnavszky F, Horváth B, Bányász T, Magyar J, Márton I, Nánási PP. Role of action potential configuration and the contribution of Ca^{2+} and K^+ currents to isoprenaline-induced changes in canine ventricular cells. *Br J Pharmacol*. 2012;167:599–611. doi: 10.1111/j.1476-5381.2012.02015.x

Circulation Research
FIRST PROOF ONLY

Downloaded from http://ahajournals.org by on April 7, 2026

44. Endoh M, Blinks JR. Actions of sympathomimetic amines on the Ca^{2+} transients and contractions of rabbit myocardium: reciprocal changes in myofibrillar responsiveness to Ca^{2+} mediated through α- and β-adrenoceptors. *Circ Res*. 1988;62:247–265. doi: 10.1161/01.res.62.2.247
45. Gao BX, Abi-Gerges N, Truong K, Stafford A, Nguyen W, Sutherland W, Vargas HM, Qu Y. Assessment of sarcomere shortening and calcium transient in primary human and dog ventricular myocytes. *J Pharmacol Toxicol Methods*. 2023;123:107278. doi: 10.1016/j.vascn.2023.107278
46. Hasenfuss G, Mulieri LA, Leavitt BJ, Alpert NR. Influence of isoproterenol on contractile protein function, excitation-contraction coupling, and energy turnover of isolated nonfailing human myocardium. *J Mol Cell Cardiol*. 1994;26:1461–1469. doi: 10.1006/jmcc.1994.1165
47. Janssen PML, Lehnart SE, Prestle J, Hasenfuss G. Preservation of contractile characteristics of human myocardium in multi-day cell culture. *J Mol Cell Cardiol*. 1999;31:1419–1427. doi: 10.1006/jmcc.1999.0978
48. Linde C, Bongiorni MG, Birgersdotter-Green U, Curtis AB, Deisenhofer I, Furokawa T, Gillis AM, Haugaa KH, Lip GYH, Van Gelder I, et al. Sex differences in cardiac arrhythmia: a consensus document of the European Heart Rhythm Association, endorsed by the Heart Rhythm Society and Asia Pacific Heart Rhythm Society. *Europace*. 2018;20:1565–1565ao. doi: 10.1093/europace/euy067
49. Yang PC, Clancy CE. In silico prediction of sex-based differences in human susceptibility to cardiac ventricular tachyarrhythmias. *Front Physiol*. 2012;3:360. doi: 10.3389/fphys.2012.00360
50. Peirlinck M, Sahli Costabal F, Kuhl E. Sex differences in drug-induced arrhythmogenesis. *Front Physiol*. 2021;12:708435. doi: 10.3389/fphys.2021.708435
51. Holmes M, Wang ZJ, Doste R, Camps J, Martinez-Navarro H, Smith H, Tomek J, Rodriguez B. Sex-specific human electromechanical multiscale in-silico models for virtual therapy evaluation. *J Mol Cell Cardiol Plus*. 2025;13:100479. doi: 10.1016/j.jmccpl.2025.100479
52. Curl CL, Wendt IR, Kotsanas G. Effects of gender on intracellular [Ca2+] in rat cardiac myocytes. *Pflugers Arch*. 2001;441:709–716. doi: 10.1007/s004240000473
53. Farrell SR, Ross JL, Howlett SE. Sex differences in mechanisms of cardiac excitation-contraction coupling in rat ventricular myocytes. *Am J Physiol Heart Circ Physiol*. 2010;299:H36–H45. doi: 10.1152/ajpheart.00299.2010
54. Guo D, Liu Q, Liu T, Elliott G, Gingras M, Kowey PR, Yan GX. Electrophysiological properties of HBI-3000: a new antiarrhythmic agent with multiple-channel blocking properties in human ventricular myocytes. *J Cardiovasc Pharmacol*. 2011;57:79–85. doi: 10.1097/FJC.0b013e3181ffe8b3
55. Sims C, Reisenweber S, Viswanathan PC, Choi BR, Walker WH, Salama G. Sex, age, and regional differences in L-type calcium current are important determinants of arrhythmia phenotype in rabbit hearts with drug-induced long QT type 2. *Circ Res*. 2008;102:e86–100. doi: 10.1161/CIRCRESAHA.108.173740
56. Vandersickel N, Van Nieuwenhuyse E, Seemann G, Panfilov AV. Spatial patterns of excitation at tissue and whole organ level due to early afterdepolarizations. *Front Physiol*. 2017;8:404. doi: 10.3389/fphys.2017.00404
57. Lehmann MH, Hardy S, Archibald D, Quart B, MacNeil DJ. Sex difference in risk of torsade de pointes with d,l-sotalol. *Circulation*. 1996;94:2535–2541. doi: 10.1161/01.cir.94.10.2535
58. Papp R, Bett GCL, Lis A, Rasmusson RL, Baczkó I, Varró A, Salama G. Genomic upregulation of cardiac Cav1.2α and NCX1 by estrogen in women. *Biol Sex Differ*. 2017;8:1–11. doi: 10.1186/s13293-017-0148-4
59. Xie LH, Weiss JN. Arrhythmogenic consequences of intracellular calcium waves. *Am J Physiol Heart Circ Physiol*. 2009;297:H997–H1002. doi: 10.1152/ajpheart.00390.2009
60. Hoeker GS, Katra RP, Wilson LD, Plummer BN, Laurita KR. Spontaneous calcium release in tissue from the failing canine heart. *Am J Physiol Heart Circ Physiol*. 2009;297:H1235–H1242. doi: 10.1152/ajpheart.01320.2008
61. Colman MA, Alvarez-Lacalle E, Echebarria B, Sato D, Sutanto H, Heijman J. Multi-scale computational modeling of spatial calcium handling from nanodomain to whole-heart: overview and perspectives. *Front Physiol*. 2022;13:836622. doi: 10.3389/fphys.2022.836622
62. Roshan N, Pandit R. Multiscale studies of delayed afterdepolarizations I: a comparison of two biophysically realistic mathematical models for human ventricular myocytes. 2023.
63. Voigt N, Li N, Wang Q, Wang W, Trafford AW, Abu-Taha I, Sun Q, Wieland T, Ravens U, Nattel S, et al. Enhanced sarcoplasmic reticulum Ca^{2+} leak and increased Na^{+}-Ca^{2+} exchanger function underlie delayed afterdepolarizations in patients with chronic atrial fibrillation. *Circulation*. 2012;125:2059–2070. doi: 10.1161/CIRCULATIONAHA.111.067306
64. Domeier TL, Maxwell JT, Blatter LA. β-Adrenergic stimulation increases the intra-sarcoplasmic reticulum Ca^{2+} threshold for Ca^{2+} wave generation. *J Physiol*. 2012;590:6093–6108. doi: 10.1113/jphysiol.2012.236117
65. Colman MA. Arrhythmia mechanisms and spontaneous calcium release: bi-directional coupling between re-entrant and focal excitation. *PLoS Comput Biol*. 2019;15:e1007260. doi: 10.1371/journal.pcbi.1007260
66. Weiss JN, Karma A, Shiferaw Y, Chen PS, Garfinkel A, Qu Z. From pulsus to pulseless: the saga of cardiac alternans. *Circ Res*. 2006;98:1244–1253. doi: 10.1161/01.RES.0000224540.97431.f0
67. Tanno K, Ryu S, Watanabe N, Minoura Y, Kawamura M, Asano T, Kobayashi Y, Katagiri T. Microvolt T-wave alternans as a predictor of ventricular tachyarrhythmias: a prospective study using atrial pacing. *Circulation*. 2004;109:1854–1858. doi: 10.1161/01.CIR.0000124717.77777.EC
68. Pruvot EJ, Katra RP, Rosenbaum DS, Laurita KR. Role of calcium cycling versus restitution in the mechanism of repolarization alternans. *Circ Res*. 2004;94:1083–1090. doi: 10.1161/01.RES.0000125629.72053.95
69. Koller ML, Maier SKG, Gelzer AR, Bauer WR, Meesmann M, Gilmour RF. Altered dynamics of action potential restitution and alternans in humans with structural heart disease. *Circulation*. 2005;112:1542–1548. doi: 10.1161/CIRCULATIONAHA.104.502831
70. Fukaya H, Plummer BN, Piktel JS, Wan X, Rosenbaum DS, Laurita KR, Wilson LD. Arrhythmogenic cardiac alternans in heart failure is suppressed by late sodium current blockade by ranolazine. *Heart Rhythm*. 2019;16:281–289. doi: 10.1016/j.hrthm.2018.08.033
71. Wan X, Cutler M, Song Z, Karma A, Matsuda T, Baba A, Rosenbaum DS. New experimental evidence for mechanism of arrhythmogenic membrane potential alternans based on balance of electrogenic I(NCX)/I(Ca) currents. *Heart Rhythm*. 2012;9:1698–1705. doi: 10.1016/j.hrthm.2012.06.031
72. Koller ML, Riccio ML, Gilmour RF. Dynamic restitution of action potential duration during electrical alternans and ventricular fibrillation. *Am J Physiol*. 1998;275:H1635–H1642. doi: 10.1152/ajpheart.1998.275.5.H1635
73. Wang L, Myles RC, Lee IJ, Bers DM, Ripplinger CM. Role of reduced sarcoendoplasmic reticulum Ca^{2+}-ATPase function on sarcoplasmic reticulum Ca^{2+} alternans in the intact rabbit heart. *Front Physiol*. 2021;12:656516. doi: 10.3389/fphys.2021.656516
74. Wan X, Laurita KR, Pruvot EJ, Rosenbaum DS. Molecular correlates of repolarization alternans in cardiac myocytes. *J Mol Cell Cardiol*. 2005;39:419–428. doi: 10.1016/j.yjmcc.2005.06.004
75. Tomek J, Hao G, Tomková M, Lewis A, Carr C, Paterson DJ, Rodriguez B, Bub G, Herring N. β-adrenergic receptor stimulation and alternans in the border zone of a healed infarct: an ex vivo study and computational investigation of arrhythmogenesis. *Front Physiol*. 2019;10:350. doi: 10.3389/fphys.2019.00350
76. Cutler MJ, Wan X, Laurita KR, Hajjar RJ, Rosenbaum DS. Targeted SERCA2a gene expression identifies molecular mechanism and therapeutic target for arrhythmogenic cardiac alternans. *Circ Arrhythm Electrophysiol*. 2009;2:686–694. doi: 10.1161/CIRCEP.109.863118
77. Child N, Bishop MJ, Hanson B, Coronel R, Opthof T, Boukens BJ, Walton RD, Efimov IR, Bostock J, Hill Y, et al. An activation-repolarization time metric to predict localized regions of high susceptibility to re-entry. *Heart Rhythm*. 2015;12:1644–1653. doi: 10.1016/j.hrthm.2015.04.013
78. Taggart P, Sutton P, Chalabi Z, Boyett MR, Simon R, Elliott D, Gill JS. Effect of adrenergic stimulation on action potential duration restitution in humans. *Circulation*. 2003;107:285–289. doi: 10.1161/01.cir.0000044941.13346.74
79. Nash MP, Bradley CP, Sutton PM, Clayton RH, Kallis P, Hayward MP, Paterson DJ, Taggart P. Whole heart action potential duration restitution properties in cardiac patients: a combined clinical and modelling study. *Exp Physiol*. 2006;91:339–354. doi: 10.1113/expphysiol.2005.031070
80. Árpádffy-Lovas T, Baczkó I, Baláti B, Bitay M, Jost N, Lengyel C, Nagy N, Takács J, Varró A, Virág L. Electrical restitution and its modifications by anti-arrhythmic drugs in undiseased human ventricular muscle. *Front Pharmacol*. 2020;11:1. doi: 10.3389/fphar.2020.00479
81. Orini M, Taggart P, Srinivasan N, Hayward M, Lambiase PD. Interactions between activation and repolarization restitution properties in the intact human heart: in-vivo whole-heart data and mathematical description. *PLoS One*. 2016;11:e0161765. doi: 10.1371/journal.pone.0161765
82. Pak HN, Hong SJ, Hwang GS, Lee HS, Park SW, Ahn JC, Ro YM, Kim YH. Spatial dispersion of action potential duration restitution kinetics is associated with induction of ventricular tachycardia/fibrillation in humans. *J Cardiovasc Electrophysiol*. 2004;15:1357–1363. doi: 10.1046/j.1540-8167.2004.03569.x
83. Jing L, Brownson K, Patwardhan A. Role of slow delayed rectifying potassium current in dynamics of repolarization and electrical memory in swine ventricles. *J Physiol Sci*. 2014;64:185–193. doi: 10.1007/s12576-014-0310-2

Circulation Research
IN PROOF ONLY

Downloaded from http://ahajournals.org by on April 7, 2026

84. Tolkacheva EG, Anumonwo JMB, Jalife J. Action potential duration restitution portraits of mammalian ventricular myocytes: role of calcium current. *Biophys J*. 2006;91:2735–2745. doi: 10.1529/biophysj.106.083865
85. Yamauchi S, Yamaki M, Watanabe T, Yuuki K, Kubota I, Tomoike H. Restitution properties and occurrence of ventricular arrhythmia in LQT2 type of long QT syndrome. *J Cardiovasc Electrophysiol*. 2002;13:910–914. doi: 10.1046/j.1540-8167.2002.00910.x
86. Lyon A, van Opbergen CJM, Delmar M, Heijman J, van Veen TAB. In silico identification of disrupted myocardial calcium homeostasis as proarrhythmic trigger in arrhythmogenic cardiomyopathy. *Front Physiol*. 2021;12:732573. doi: 10.3389/fphys.2021.732573
87. Srinivasan NT, Orini M, Simon RB, Providência R, Khan FZ, Segal OR, Babu GG, Bradley R, Rowland E, Ahsan S, et al. Ventricular stimulus site influences dynamic dispersion of repolarization in the intact human heart. *Am J Physiol Heart Circ Physiol*. 2016;311:H545–H554. doi: 10.1152/ajpheart.00159.2016
88. Corral-Acero J, Margara F, Marciniak M, Rodero C, Loncaric F, Feng Y, Gilbert A, Fernandes JF, Bukhari HA, Wajdan A, et al. The 'digital twin' to enable the vision of precision cardiology. *Eur Heart J*. 2020;41:4556–4564. doi: 10.1093/eurheartj/ehaa159
89. Edwards AG, Louch WE. Species-dependent mechanisms of cardiac arrhythmia: a cellular focus. *Clin Med Insights Cardiol*. 2017;11:117954681668606. doi: 10.1177/1179546816686061
90. De Bruin ML, Pettersson M, Meyboom RHB, Hoes AW, Leufkens HGM. Anti-HERG activity and the risk of drug-induced arrhythmias and sudden death. *Eur Heart J*. 2005;26:590–597. doi: 10.1093/eurheartj/ehi092
91. DeFilippis EM, Van Spall HGC. Is it time for sex-specific guidelines for cardiovascular disease? *J Am Coll Cardiol*. 2021;78:189–192. doi: 10.1016/j.jacc.2021.05.012
92. Shivkumar K, Ajijola OA, Anand I, Armour JA, Chen PS, Esler M, De Ferrari GM, Fishbein MC, Goldberger JJ, Harper RM, et al. Clinical neurocardiology defining the value of neuroscience-based cardiovascular therapeutics. *J Physiol*. 2016;594:3911–3954. doi: 10.1113/JP271870
93. Kalla M, Hao G, Tapoulal N, Tomek J, Liu K, Woodward L, Dall'Armellina E, Banning AP, Choudhury RP, Neubauer S, et al; 'Oxford Acute Myocardial Infarction (OxAMI) Study'. The cardiac sympathetic co-transmitter neuropeptide Y is pro-arrhythmic following ST-elevation myocardial infarction despite beta-blockade. *Eur Heart J*. 2020;41:2168–2179. doi: 10.1093/eurheartj/ehz852
94. Crocini C, Coppini R, Ferrantini C, Yan P, Loew LM, Tesi C, Cerbai E, Poggesi C, Pavone FS, Sacconi L. Defects in T-tubular electrical activity underlie local alterations of calcium release in heart failure. *Proc Natl Acad Sci USA*. 2014;111:15196–15201. doi: 10.1073/pnas.1411557111
95. Colman MA, Pinali C, Trafford AW, Zhang H, Kitmitto A. A computational model of spatio-temporal cardiac intracellular calcium handling with realistic structure and spatial flux distribution from sarcoplasmic reticulum and t-tubule reconstructions. *PLoS Comput Biol*. 2017;13:e1005714. doi: 10.1371/journal.pcbi.1005714
96. Rovetti R, Cui X, Garfinkel A, Weiss JN, Qu Z. Spark-induced sparks as a mechanism of intracellular calcium alternans in cardiac myocytes. *Circ Res*. 2010;106:1582–1591. doi: 10.1161/CIRCRESAHA.109.213975
97. Bueno-Orovio A, Cherry EM, Fenton FH. Minimal model for human ventricular action potentials in tissue. *J Theor Biol*. 2008;253:544–560. doi: 10.1016/j.jtbi.2008.03.029
98. Meier S, Grundland A, Dobrev D, Volders PGA, Heijman J. In silico analysis of the dynamic regulation of cardiac electrophysiology by Kv 11.1 ion-channel trafficking. *J Physiol*. 2023;601:2711–2731. doi: 10.1113/JP283976
99. Cortassa S, Juhaszova M, Aon MA, Zorov DB, Sollott SJ. Mitochondrial Ca^{2+}, redox environment and ROS emission in heart failure: two sides of the same coin? *J Mol Cell Cardiol*. 2021;151:113–125. doi: 10.1016/j.yjmcc.2020.11.013
100. Ngo K, Yang PC, Yarov-Yarovoy V, Clancy CE, Vorobyov I. Harnessing AlphaFold to reveal hERG channel conformational state secrets. *Elife*. 2024;13:RP104901. doi: 10.7554/eLife.104901
101. Bunne C, Roohani Y, Rosen Y, Gupta A, Zhang X, Roed M, Alexandrov T, AlQuraishi M, Brennan P, Burkhardt DB, et al. How to build the virtual cell with artificial intelligence: priorities and opportunities. *Cell*. 2024;187:7045–7063. doi: 10.1016/j.cell.2024.11.015
102. Hund TJ, Kucera JP, Otani NF, Rudy Y. Ionic charge conservation and long-term steady state in the Luo-Rudy dynamic cell model. *Biophys J*. 2001;81:3324–3331. doi: 10.1016/s0006-3495(01)75965-6
103. Magyar J, Iost N, Körtvély A, Bányász T, Virág L, Szigligeti P, Varró A, Opincariu M, Szécsi J, Papp JG, Nánási PP. Effects of endothelin-1 on calcium and potassium currents in undiseased human ventricular myocytes. *Pflugers Arch*. 2000;441:144–149. doi: 10.1007/s004240000400
104. Fülöp L, Bányász T, Magyar J, Szentandrássy N, Varró A, Nánási PP. Reopening of L-type calcium channels in human ventricular myocytes during applied epicardial action potentials. *Acta Physiol Scand*. 2004;180:39–47. doi: 10.1046/j.0001-6772.2003.01223.x
105. He H, Meyer M, Martin JL, McDonough PM, Ho P, Lou X, Lew WYW, Hilal-Dandan R, Dillmann WH. Effects of mutant and antisense RNA of phospholamban on SR Ca^{2+}-ATPase activity and cardiac myocyte contractility. *Circulation*. 1999;100:974–980. doi: 10.1161/01.cir.100.9.974
106. Ko CY, Liu MB, Song Z, Qu Z, Weiss JN. Multiscale determinants of delayed afterdepolarization amplitude in cardiac tissue. *Biophys J*. 2017;112:1949–1961. doi: 10.1016/j.bpj.2017.03.006
107. Wilson LD, Jeyaraj D, Wan X, Hoeker GS, Said TH, Gittinger M, Laurita KR, Rosenbaum DS. Heart failure enhances susceptibility to arrhythmogenic cardiac alternans. *Heart Rhythm*. 2009;6:251–259. doi: 10.1016/j.hrthm.2008.11.008
108. Gardner R, Wang L, Lang B, Cregg J, Dunbar C, Woodward W, Silver J, Ripplinger C, Habecker B. Targeting protein tyrosine phosphatase sigma after myocardial infarction restores cardiac sympathetic innervation and prevents arrhythmias. *Nat Commun*. 2015;6:6235. doi: 10.1038/ncomms7235
109. Stary V, Puppala D, Scherrer-Crosbie M, Dillmann WH, Armoundas AA. SERCA2a upregulation ameliorates cellular alternans induced by metabolic inhibition. *J Appl Physiol (1985)*. 2016;120:865–875. doi: 10.1152/japplphysiol.00588.2015
110. Xie LH, Sato D, Garfinkel A, Qu Z, Weiss JN. Intracellular Ca alternans: coordinated regulation by sarcoplasmic reticulum release, uptake, and leak. *Biophys J*. 2008;95:3100–3110. doi: 10.1529/biophysj.108.130955
111. Kameyama M, Hirayama Y, Saitoh H, Maruyama M, Atarashi H, Takano T. Possible contribution of the sarcoplasmic reticulum Ca^{2+} pump function to electrical and mechanical alternans. *J Electrocardiol*. 2003;36:125–135. doi: 10.1054/jelc.2003.50021
112. Bhattacharyya ML, Vassalle M. Effects of tetrodotoxin on electrical and mechanical activity of cardiac Purkinje fibers. *J Electrocardiol*. 1982;15:351–360. doi: 10.1016/s0022-0736(82)81008-x
113. Tucker CR, Winkle RA, Peters FA, Harrison DC. Acute hemodynamic effects of intravenous encainide in patients with heart disease. *Am Heart J*. 1982;104:209–215. doi: 10.1016/0002-8703(82)90194-6
114. Gottlieb SS, Kukin ML, Medina N, Yushak M, Packer M. Comparative hemodynamic effects of procainamide, tocainide, and encainide in severe chronic heart failure. *Circulation*. 1990;81:860–864. doi: 10.1161/01.cir.81.3.860
115. Pieske B, Maier LS, Piacentino V, Weisser J, Hasenfuss G, Houser S. Rate dependence of $[Na^+]_i$ and contractility in nonfailing and failing human myocardium. *Circulation*. 2002;106:447–453. doi: 10.1161/01.cir.0000023042.50192.f4
116. Rautaharju P, Zhou SH, Wong S, Calhoun H, Berenson G, Prineas R, Davignon A. Sex differences in the evolution of the electrocardiographic QT interval with age. *Can J Cardiol*. 1992;8:690–695.
117. Salama G, Bett GCL. Sex and gender differences in cardiovascular physiology–back to basics: sex differences in the mechanisms underlying long QT syndrome. *Am J Physiol Heart Circ Physiol*. 2014;307:H640–H648. doi: 10.1152/ajpheart.00864.2013
118. Fogli Iseppe A, Ni H, Zhu S, Zhang X, Coppini R, Yang PC, Srivatsa U, Clancy CE, Edwards AG, Morotti S, et al. Sex-specific classification of drug-induced torsade de pointes susceptibility using cardiac simulations and machine learning. *Clin Pharmacol Ther*. 2021;110:380–391. doi: 10.1002/cpt.2240
119. Pham TV, Sosunov EA, Gainullin RZ, Danilo P, Rosen MR. Impact of sex and gonadal steroids on prolongation of ventricular repolarization and arrhythmias induced by Ik-blocking drugs. *Circulation*. 2001;103:2207–2212. doi: 10.1161/01.cir.103.17.2207
120. Ng GA, Brack KE, Patel VH, Coote JH. Autonomic modulation of electrical restitution, alternans and ventricular fibrillation initiation in the isolated heart. *Cardiovasc Res*. 2007;73:750–760. doi: 10.1016/j.cardiores.2006.12.001
121. Winter J, Bishop MJ, Wilder CDE, O'Shea C, Pavlovic D, Shattock MJ. Sympathetic nervous regulation of calcium and action potential alternans in the intact heart. *Front Physiol*. 2018;9:16. doi: 10.3389/fphys.2018.00016
122. Cranefield PF. Action potentials, afterpotentials, and arrhythmias. *Circ Res*. 1977;41:415–423. doi: 10.1161/01.res.41.4.415

ORIGINAL RESEARCH

Downloaded from http://ahajournals.org by on April 7, 2026

Circulation Research
THIS PROOF ONLY

123. Ferrier GR, Saunders JH, Mendez C. A cellular mechanism for the generation of ventricular arrhythmias by acetylstrophanthidin. *Circ Res*. 1973;32:600–609. doi: 10.1161/01.res.32.5.600
124. Venetucci LA, Trafford AW, Eisner DA. Increasing ryanodine receptor open probability alone does not produce arrhythmogenic calcium waves: threshold sarcoplasmic reticulum calcium content is required. *Circ Res*. 2007;100:105–111. doi: 10.1161/01.RES.0000252828.17939.00
125. Doste R, Coppini R, Bueno-Orovio A. Remodelling of potassium currents underlies arrhythmic action potential prolongation under beta-adrenergic stimulation in hypertrophic cardiomyopathy. *J Mol Cell Cardiol*. 2022;172:120–131. doi: 10.1016/j.yjmcc.2022.08.361
126. Baba S, Dun W, Boyden PA. Can PKA activators rescue Na^+ channel function in epicardial border zone cells that survive in the infarcted canine heart? *Cardiovasc Res*. 2004;64:260–267. doi: 10.1016/j.cardiores.2004.06.021
127. Horváth B, Hézső T, Szentandrássy N, Kistamás K, Árpádffy-Lovas T, Varga R, Gazdag P, Veress R, Dienes C, Baranyai D, et al. Late sodium current in human, canine and guinea pig ventricular myocardium. *J Mol Cell Cardiol*. 2020;139:14–23. doi: 10.1016/j.yjmcc.2019.12.015
128. Nagykaldi Z, Kem D, Lazzara R, Szabo B. Canine ventricular myocyte β2-adrenoceptors are not functionally coupled to L-type calcium current. *J Cardiovasc Electrophysiol*. 1999;10:1240–1251. doi: 10.1111/j.1540-8167.1999.tb00302.x
129. Papa A, Zakharov SI, Katchman AN, Kushner JS, Chen B, Yang L, Liu G, Jimenez AS, Eisert RJ, Bradshaw GA, et al. Rad regulation of $Ca_V1.2$ channels controls cardiac fight-or-flight response. *Nat Cardiovasc Res*. 2022;1:1022–1038. doi: 10.1038/s44161-022-00157-y
130. Cordeiro JM, Greene L, Heilmann C, Antzelevitch D, Antzelevitch C. Transmural heterogeneity of calcium activity and mechanical function in the canine left ventricle. *Am J Physiol Heart Circ Physiol*. 2004;286:H1471–H1479. doi: 10.1152/ajpheart.00748.2003
131. Bartos DC, Morotti S, Ginsburg KS, Grandi E, Bers DM. Quantitative analysis of the Ca^{2+} -dependent regulation of delayed rectifier K^+ current IKs in rabbit ventricular myocytes. *J Physiol*. 2017;595:2253–2268. doi: 10.1113/JP273676
132. Liu DW, Antzelevitch C. Characteristics of the delayed rectifier current (IKr and IKs) in canine ventricular epicardial, midmyocardial, and endocardial myocytes. A weaker IKs contributes to the longer action potential of the M cell. *Circ Res*. 1995;76:351–365. doi: 10.1161/01.res.76.3.351
133. Banyasz T, Jian Z, Horvath B, Khabbaz S, Izu LT, Chen-Izu Y. Beta-adrenergic stimulation reverses the IKr–IKs dominant pattern during cardiac action potential. *Pflugers Arch*. 2014;466:2067–2076. doi: 10.1007/s00424-014-1465-7
134. Carro J, Rodríguez JF, Laguna P, Pueyo E. A human ventricular cell model for investigation of cardiac arrhythmias under hyperkalaemic conditions. *Philos Trans A Math Phys Eng Sci*. 2011;369:4205–4232. doi: 10.1098/rsta.2011.0127
135. Wang W, Landstrom AP, Wang Q, Munro ML, Beavers D, Ackerman MJ, Soeller C, Wehrens XHT. Reduced junctional Na^+/Ca^{2+}-exchanger activity contributes to sarcoplasmic reticulum Ca^{2+} leak in junctophilin-2-deficient mice. *Am J Physiol Heart Circ Physiol*. 2014;307:H1317–H1326. doi: 10.1152/ajpheart.00413.2014
136. Weiss JN, Qu Z, Shivkumar K. The electrophysiology of hypo- and hyperkalemia. *Circ Arrhythm Electrophysiol*. 2017;10:e004667. doi: 10.1161/CIRCEP.116.004667
137. Despa S, Bossuyt J, Han F, Ginsburg KS, Jia LG, Kutchai H, Tucker AL, Bers DM. Phospholemman-phosphorylation mediates the beta-adrenergic effects on Na/K pump function in cardiac myocytes. *Circ Res*. 2005;97:252–259. doi: 10.1161/01.RES.0000176532.97731.e5
138. Nakao M, Gadsby DC. [Na] and [K] dependence of the Na/K pump current-voltage relationship in guinea pig ventricular myocytes. *J Gen Physiol*. 1989;94:539–565. doi: 10.1085/jgp.94.3.539
139. Wehrens XHT. CaMKII regulation of the cardiac ryanodine receptor and SR calcium release. *Heart Rhythm*. 2011;8:323. doi: 10.1016/j.hrthm.2010.09.079
140. Laurita KR, Katra R, Wible B, Wan X, Koo MH. Transmural heterogeneity of calcium handling in canine. *Circ Res*. 2003;92:668–675. doi: 10.1161/01.RES.0000062468.25308.27
141. Huke S, Bers DM. Temporal dissociation of frequency-dependent acceleration of relaxation and protein phosphorylation by CaMKII. *J Mol Cell Cardiol*. 2007;42:590–599. doi: 10.1016/j.yjmcc.2006.12.007
142. Picht E, DeSantiago J, Huke S, Kaetzel MA, Dedman JR, Bers DM. CaMKII inhibition targeted to the sarcoplasmic reticulum inhibits frequency-dependent acceleration of relaxation and Ca^{2+} current facilitation. *J Mol Cell Cardiol*. 2007;42:196–205. doi: 10.1016/j.yjmcc.2006.09.007
143. Soltis AR, Saucerman JJ. Synergy between CaMKII substrates and β-adrenergic signaling in regulation of cardiac myocyte Ca2 handling. *Biophys J*. 2010;99:2038–2047. doi: 10.1016/j.bpj.2010.08.016
144. Negroni JA, Morotti S, Lascano EC, Gomes AV, Grandi E, Puglisi JL, Bers DM. β-adrenergic effects on cardiac myofilaments and contraction in an integrated rabbit ventricular myocyte model. *J Mol Cell Cardiol*. 2015;81:162–175. doi: 10.1016/j.yjmcc.2015.02.014
145. Yue DT. Intracellular $[Ca^{2+}]$ related to rate of force development in twitch contraction of heart. *Am J Physiol*. 1987;252:H760. doi: 10.1152/ajpheart.1987.252.4.H760
146. Marban E, Kusuoka H, Yue DT, Weisfeldt ML, Wier WG. Maximal Ca^{2+}-activated force elicited by tetanization of ferret papillary muscle and whole heart: mechanism and characteristics of steady contractile activation in intact myocardium. *Circ Res*. 1986;59:262–269. doi: 10.1161/01.res.59.3.262
147. Davis JP, Norman C, Kobayashi T, Solaro RJ, Swartz DR, Tikunova SB. Effects of thin and thick filament proteins on calcium binding and exchange with cardiac troponin C. *Biophys J*. 2007;92:3195–3206. doi: 10.1529/biophysj.106.095406
148. Rao V, Cheng Y, Lindert S, Wang D, Oxenford L, McCulloch AD, McCammon JA, Regnier M. PKA phosphorylation of cardiac troponin I modulates activation and relaxation kinetics of ventricular myofibrils. *Biophys J*. 2014;107:1196–1204. doi: 10.1016/j.bpj.2014.07.027
149. Okazaki O, Suda N, Hongo K, Konishi M, Kurihara S. Modulation of Ca^{2+} transients and contractile properties by beta-adrenoceptor stimulation in ferret ventricular muscles. *J Physiol*. 1990;423:221–240. doi: 10.1113/jphysiol.1990.sp018019
150. Herron TJ, Korte FS, McDonald KS. Power output is increased after phosphorylation of myofibrillar proteins in rat skinned cardiac myocytes. *Circ Res*. 2001;89:1184–1190. doi: 10.1161/hh2401.101908
151. Flórez-Vargas O, Brass A, Karystianis G, Bramhall M, Stevens R, Cruickshank S, Nenadic G. Bias in the reporting of sex and age in biomedical research on mouse models. *Elife*. 2016;5:e13615. doi: 10.7554/eLife.13615
152. Vitale C, Fini M, Spoletini I, Lainscak M, Seferovic P, Rosano GM. Under-representation of elderly and women in clinical trials. *Int J Cardiol*. 2017;232:216–221. doi: 10.1016/j.ijcard.2017.01.018
153. Gaborit N, Varro A, Le Bouter S, Szuts V, Escande D, Nattel S, Demolombe S. Gender-related differences in ion-channel and transporter subunit expression in non-diseased human hearts. *J Mol Cell Cardiol*. 2010;49:639–646. doi: 10.1016/j.yjmcc.2010.06.005
154. Chu SH, Sutherland K, Beck J, Kowalski J, Goldspink P, Schwertz D. Sex differences in expression of calcium-handling proteins and beta-adrenergic receptors in rat heart ventricle. *Life Sci*. 2005;76:2735–2749. doi: 10.1016/j.lfs.2004.12.013
155. Britton OJ, Bueno-Orovio A, Virág L, Varró A, Rodriguez B. The electrogenic Na^+/K^+ pump is a key determinant of repolarization abnormality susceptibility in human ventricular cardiomyocytes: a population-based simulation study. *Front Physiol*. 2017;8:278. doi: 10.3389/fphys.2017.00278
156. Clerx M, Collins P, de Lange E, Volders PGA. Myokit: a simple interface to cardiac cellular electrophysiology. *Prog Biophys Mol Biol*. 2016;120:100–114. doi: 10.1016/j.pbiomolbio.2015.12.008
157. Pitt-Francis J, Pathmanathan P, Bernabeu MO, Bordas R, Cooper J, Fletcher AG, Mirams GR, Murray P, Osborne JM, Walter A, et al. Chaste: a test-driven approach to software development for biological modelling. *Comput Phys Commun*. 2009;180:2452–2471. doi: 10.1098/rsta.2008.0096
158. Sachetto Oliveira R, Martins Rocha B, Burgarelli D, Meira W, Constantinides C, Weber dos Santos R. Performance evaluation of GPU parallelization, space-time adaptive algorithms, and their combination for simulating cardiac electrophysiology. *Int J Numer Method Biomed Eng*. 2018;34:e2913. doi: 10.1002/cnm.2913
159. Bartolucci C, Passini E, Hyttinen J, Paci M, Severi S. Simulation of the effects of extracellular calcium changes leads to a novel computational model of human ventricular action potential with a revised calcium handling. *Front Physiol*. 2020;11:314. doi: 10.3389/fphys.2020.00314
160. Morales D, Hermosilla T, Varela D. Calcium-dependent inactivation controls cardiac L-type Ca^{2+} currents under β-adrenergic stimulation. *J Gen Physiol*. 2019;151:786–797. doi: 10.1085/jgp.201812236
161. Pogwizd SM, Onufer JR, Kramer JB, Sobel BE, Corr PB. Induction of delayed afterdepolarizations and triggered activity in canine Purkinje fibers by lysophosphoglycerides. *Circ Res*. 1986;59:416–426. doi: 10.1161/01.res.59.4.416
162. Brochet DXP, Yang D, Di Maio A, Lederer WJ, Franzini-Armstrong C, Cheng H. Ca^{2+} blinks: rapid nanoscopic store calcium signaling. *Proc Natl Acad Sci USA*. 2005;102:3099–3104. doi: 10.1073/pnas.0500059102

Downloaded from http://ahajournals.org by on April 7, 2026

Circulation Research
FIRST PROOF ONLY

163. Tomek J, Tomková M, Zhou X, Bub G, Rodriguez B. Modulation of cardiac alternans by altered sarcoplasmic reticulum calcium release: a simulation study. *Front Physiol.* 2018;9:1306. doi: 10.3389/fphys.2018.01306
164. Bassani JW, Yuan W, Bers DM. Fractional SR Ca release is regulated by trigger Ca and SR Ca content in cardiac myocytes. *Am J Physiol.* 1995;268:C1313–C1319. doi: 10.1152/ajpcell.1995.268.5.C1313
165. Yue AM, Franz MR, Roberts PR, Morgan JM. Global endocardial electrical restitution in human right and left ventricles determined by noncontact mapping. *J Am Coll Cardiol.* 2005;46:1067–1075. doi: 10.1016/j.jacc.2005.05.074
166. Glukhov AV, Fedorov VV, Kalish PW, Ravikumar VK, Lou Q, Janks D, Schuessler RB, Moazami N, Efimov IR. Conduction remodeling in human end-stage non-ischemic left ventricular cardiomyopathy. *Circulation.* 2012;125:1835–1847. doi: 10.1161/CIRCULATIONAHA.111.047274
167. Lou Q, Janks DL, Holzem KM, Lang D, Onal B, Ambrosi CM, Fedorov VV, Wang IW, Efimov IR. Right ventricular arrhythmogenesis in failing human heart: the role of conduction and repolarization remodeling. *Am J Physiol Heart Circ Physiol.* 2012;303:H1426–H1434. doi: 10.1152/ajpheart.00457.2012

American Heart Association.
Circulation Research
FIRST PROOF ONLY

Downloaded from http://ahajournals.org by on April 7, 2026